Agenzia nazionale per le nuove tecnologie,
l'energia e lo sviluppo economico sostenibile

MINISTERO DELLO SVILUPPO ECONOMICO

Raccolta delle principali attività di diffusione dei risultati del Progetto D.3 "Processi e macchinari industriali" PAR2015

A cura di I. Bertini

Report RdS/PAR2015/074

RELAZIONE SINTETICA DELL'ATTIVITÀ DI COLLABORAZIONE CON IL POLITECNICO DI TORINO SULLE TECNICHE DI EFFICIENTAMENTO PER SISTEMI DI MICROCOGENERAZIONE

A cura di I. Bertini (ENEA)

Settembre 2016

Report Ricerca di Sistema Elettrico
Accordo di Programma Ministero dello Sviluppo Economico - ENEA
Piano Annuale di Realizzazione 2015
Area: : Efficienza energetica e risparmio di energia negli usi finali elettrici e interazione con altri vettori energetici
Progetto: Processi e macchinari industriali
Obiettivo: A. Studio e applicazione di tecnologie per l'efficientamento di macchinari

Responsabile del Progetto: Ing. Ilaria Bertini, ENEA

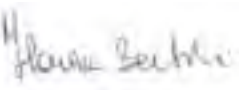

Indice

Introduzione

Il Ministero dello Sviluppo Economico (MiSE) ed ENEA hanno stipulato un Accordo di Programma in base al quale è concesso il contributo finanziario per l'esecuzione delle linee di attività del Piano Triennale della Ricerca e Sviluppo 2015-2017 di interesse generale per il Sistema Elettrico Nazionale.

Il presente documento si riferisce al Piano Annuale di Realizzazione 2015, per quanto attiene all'Area "Efficienza energetica e risparmio di energia negli usi finali elettrici e interazione con altri vettori energetici", Progetto D.3 "Processi e macchinari industriali".

Il periodo di svolgimento delle attività è 1 ottobre 2015 - 30 settembre 2016.

Il progetto ha come la realizzazione di strumenti e metodi, che mirano alla promozione di tecnologie ad alta efficienza energetica, allo scopo di favorire il mercato di prodotti più performanti sia a livello di componenti, che consumano energia, sia a livello di sistemi che la producono e di migliorare la qualità dei processi industriali più energivori per contribuire alla riduzione della bolletta energetica nazionale e aumentare la competitività del settore produttivo rispetto ai mercati internazionali.

L'attività a termine, con un orizzonte temporale triennale, si articola attraverso le seguenti cinque linee di attività, più una dedicata alla diffusione dei contenuti e dei risultati ottenuti.

a. **Studio e applicazione di tecnologie per l'efficientamento di macchinari**

- *Facility per la sperimentazione e verifica di motori elettrici ad alta efficienza*

  Obiettivo di questa linea di attività è il potenziamento di una struttura (progettata e in parte allestita nel piano triennale 2012-2014, sede ENEA di Bologna) per la sperimentazione e verifica del motori elettrici fino a 55kW. Allo scopo di definire i protocolli di misura (attualmente non disponibili) necessari per attuare la verifica dei motori come previsto dal sistema di sorveglianza del mercato, si elaborerà un metodo per la validazione dei risultati basato sull'analisi delle incertezze di misura.

- *Tecniche di efficientamento per sistemi di microcogenerazione*

  L'attività ha l'obiettivo di analizzare l'impatto della normativa inerente i SEU sugli scenari di applicazione della micro cogenerazione per evidenziare i vantaggi in termini costi/benefici ad essa correlati. Numerosi sono stati gli stimoli da parte di imprese produttrici di tale tecnologia ad avviare un approfondimento dello studio del possibile efficientamento delle sue applicazioni reali. Si prevede lo sviluppo di strumenti di modellazione matematica che consentano di proporre opportunità di miglioramento dell'efficienza delle applicazioni reali della micro cogenerazione e la predisposizione (progettazione e approvvigionamento di un sistema di monitoraggio ad hoc) di una campagna sperimentale in campo presso un sito da individuare in collaborazione con un'azienda produttrice del settore, che consenta di caratterizzarne le principali criticità.

- *La progettazione ecocompatibile all'interno dell'economia circolare*

  Obiettivo di questa linea è lo sviluppo di specifiche e requisiti tecnici per le politiche di efficienza energetica, principalmente etichettatura energetica- ecoprogettazione (ecodesign)

all'interno del cosiddetto pacchetto dell' "economia circolare". A livello nazionale è essenziale garantire l'attuazione (definizione, monitoraggio e controllo) dell'etichettatura e dei requisiti di ecoprogettazione, monitorando la reale presenza delle etichette nei negozi e verificando la conformità dei prodotti immessi sul mercato ai requisiti di legge. In questo modo si proteggono i consumatori e l'industria nazionale dalla concorrenza sleale. Le azioni previste nell'annualità si focalizzeranno su prodotti industriali, professionali e domestici, per identificare i modelli a più elevata ecoefficienza e permetterne la loro diffusione/commercializzazione; inoltre verrà verificata la presenza delle etichette energetiche nei punti vendita dei prodotti di largo consumo, mediante un'indagine realizzata da una società di analisi del mercato in un campione di negozi in tutto il Paese.

b. **Efficientamento di processi industriali**

- *Materiali innovativi per lo sviluppo di sistemi per il recupero energetico da cascami termici in ambito industriale*

  L'obiettivo finale di questa linea di attività nell'orizzonte temporale triennale è lo sviluppo di un sistema prototipale ad assorbimento o adsorbimento per il recupero di calore di scarto a bassa temperatura. L'attività del primo anno è finalizzata all'individuazione di materiali a basso costo da utilizzare quali substrati solidi assorbenti e/o adsorbenti in grado di permettere recuperi energetici a partire da cascami termici a bassa temperatura. In parallelo verrà sviluppato un nuovo ciclo frigorifero a ciclo aperto in cui i materiali individuati verranno utilizzati quale stadio ad adsorbimento.

- *Studio di catalizzatori magnetici a elevata attività con finalità di efficientamento energetico dei processi produttivi nell'industria chimica*

  L'attività mira alla progettazione e sviluppo di nuovi catalizzatori a supporto magnetico da utilizzare ai fini dell'efficientamento energetico di processi produttivi in ambito chimico industriale, con particolare focalizzazione al sistema nazionale (chimica farmaceutica, petrolchimico, sintesi di materie plastiche, sviluppo di coatings, prodotti avanzati per l'edilizia…). L'obiettivo finale nell'orizzonte temporale triennale del Programma consiste nell'allestimento di un reattore a scala di laboratorio per la sperimentazione di nuovi materiali (catalizzatori) da utilizzare nella catalisi magnetica per induzione, tecnica che si configura come *game changer* nel settore della chimica industriale. D'altra parte, l'efficacia di tale tecnologia in termini di risparmio energetico è strettamente legata al design dei catalizzatori e alla loro caratterizzazione chimico-fisica e funzionale. Tali servizi tecnico-scientifici potranno essere resi disponibili attraverso la predisposizione della struttura (reattore) obiettivo finale del presente task.

- *Sistema di supporto alle decisioni per il risparmio energetico nella produzione e nell'utilizzazione dell'aria compressa*

  Obiettivo finale della presente linea, nell'orizzonte temporale triennale, è la definizione di metodi per la riduzione dei consumi degli impianti di produzione, trattamento, distribuzione e utilizzo dell'aria compressa e la realizzazione di uno strumento di supporto alle decisioni (DSS, Decision Support Systems) in grado di indirizzare le aziende di vari settori produttivi verso l'adozione di tali buone pratiche secondo le modalità e le specifiche esigenze del settore e dell'impianto. Le attività della prima annualità saranno orientate all'Individuazione dei principali campi di applicazione sul territorio italiano, analisi dell'uso dell'aria compressa

nelle aziende italiane nei diversi settori produttivi e dello stato dell'arte per quanto riguarda l'efficientamento energetico di tali impianti e lo sviluppo di un modello di maturità che, utilizzato in modalità di self-assessment, sia in grado di fornire alle aziende una fotografia del loro stato attuale di avanzamento in tale ambito e quindi le aiuti a delineare un adeguato percorso di sviluppo.

c. **Metodologie per la caratterizzazione di processi industriali energivori: benchmark e valutazione dei potenziali di risparmio energetico**

Obiettivo delle attività del primo anno è l'analisi puntuale e statistica delle diagnosi energetiche predisposte dalle aziende. Ciò permetterà di individuare tra gli indici di prestazione più significativi di processo nel settore industriale e di individuare le tecnologie maggiormente adoperate nei vari settori merceologici caratterizzandone in modo più puntuale gli aspetti energetici. In collaborazione con le associazioni di categoria e con i principali players dei vari settori industriali, si valuterà il potenziale di risparmio energetico di tre settori specifici opportunamente scelti, ovvero il settore ceramico, quello metallurgico/siderurgico e cartario. Si intende anche valutare l'impatto potenziale derivante dall'implementazione di strumenti tecnico-finanziari (diagnosi energetica, rete d'impresa, ecc.) all'interno di PMI del settore industriale, in termini di risparmio energetico e costi da sostenere per l'esecuzione dei necessari interventi di efficientamento.

d. **Impiego di tecnologie elettriche nei processi industriali**

- *Efficientamento dei processi di saldatura industriale*

L'obiettivo finale della presente linea di attività la definizione di uno standard di verifica dei consumi energetici normalizzati per l'etichettatura di vari generatori di energia per saldatura e la predisposizione di linee guida per il risparmio energetico nel settore della saldatura Industriale. Allo stato attuale tali specifiche tecniche non sono disponibili. In tal senso si rende necessario allestire un laboratorio di misura e verifica delle principali tecniche utilizzate nel settore industriale per effettuare le saldature. In particolare, sarà potenziato unl sistema di saldatura laser ad alta efficienza con componenti optoelettronici (acquisito nel precedente piano triannale) in grado di incrementare l'attuale potenza da 2300 W a 4000 W per garantire l'applicazione del processo in almeno due range di produttività sullo spessore di 5 mm di spessore. Le azioni principali del primo anno saranno indirizzate alla definizione delle condizioni di testing per la valutazione dell'efficienza energetica delle tecnologie di saldatura Elecron Beam (EBW), Laser (LBW) a arco ad elettrodo infusibile "Tungsten inert gas Welding" (TIG) e Friction Stir Welding (FSW).

- *Applicazione di campi elettrici pulsati (PEF) nei processi industriali*

In tale contesto si propone un'attività volta ad affrontare complessi problemi di trattamento di inattivazione batterica di sostanze, liquide e gassose, con il vantaggio di una affidabilità ineguagliata dalle altre tecnologie e ella prospettiva di applicabilità di questa tecnica su larga scala, dalla valorizzazione energetica degli scarti industriali alla lavorazione di prodotti di utilità collettiva (conservazione dei prodotti alimentari) in sostituzione delle attuali tecniche (tradizionali metodi termici), più dispendiose da un punto di vista della efficienza energetica.

La prima fase del progetto consisterà nell'individuazione degli ambiti e dei criteri di applicazione. In particolare, per il settore alimentare l'attività sarà rivolta a definire un quadro di dettaglio sulla sicurezza alimentare e sui potenziali di risparmi energetico stimabili. Successivamente si passerà al processamento dei dati acquisiti, al fine di indicare e definire i criteri di progettazione sia generici e sia specifici in base al contesto di applicazione per la realizzazione di sistema da sperimentare in campo. Questa sarà sicuramente la fase più complessa in quanto gli attuali studi trattano l'argomento in modo estremamente eterogeneo applicando i PEF a casi specifici.

e. **Tecnologie ICT per l'efficientamento dei processi industriali**

Progettazione di una rete di sensori e attuatori wireless basata su protocolli machine-to-machine (M2M) e finalizzata alla riduzione dei consumi energetici degli impianti industriali. Le attività del primo anno saranno mirate alla risoluzione di importanti problematiche tecniche ancora irrisolte quali la sicurezza della trasmissione dei dati (cyber-security) e la non predicibilità di comportamento dovuta all'enorme quantitativo di variabili che entrano in gioco (interferenze, interazione con l'ambiente,ecc.).

Nel presente documento è stato collezionato il materiale delle principali azioni di diffusione dei risultati relative alle attività del PAR 2015 dei ricercatori ENEA e cobeneficiari.

1 Pubblicazioni scientifiche

Obiettivo b

1. "Nanostructured metal hydride e Polymer composite as fixed bed for sorption technologies. Advantages of an innovative combined approach by high-energy ball milling and extrusion techniques", Marzia Pentimalli, Enrico Imperi, Alessandro Zaccagnini, Franco Padella, Renewable Energy, ELSEVIER, 2016.
2. "Assessing and improving Compressed Air Systems' energy efficiency in production and use: findings from an explorative study in large and energy-intensive industrial firms ", Miriam Benedetti, Ilaria Bertini, Francesca Bonfà, Silvia Ferrari, Vito Introna, Domenico Santino, Stefano Ubertini, accettato al ICAE (International Conference on Applied Energy), Beijing, China, october 8-11, 2016.
3. "Solving compressed air systems' energy puzzle: how does your system stack up?" , Miriam Benedetti, Francesca Bonfà, Vito Introna, EPSRC Centre for Industrial Sustainability annual Conference, University of Cambridge, 7-8-July 2016

Obiettivo c

4. Nardin G., Simeoni P., Alvarez Y, Pozzetto D. - Modelo de Planificación Energética Territorial desde la óptica de la Green y Lean , V Congreso Nacional de Ingenieria, Ciencias y Tecnologia" Università Tecnologica de Panamá, 2015.
5. Ciotti G., Meneghetti A., Nardin G., Simeoni P. "Fostering sustainable micro district heating: a tool for biomass boiler design" XI Summer School "Francesco Turco", September 13–15, 2016 .
6. Annicchiarico B., Correani L., Di Dio F. (2016), Environmental Policy and Endogenous Market Structure. CEIS Research paper 14(8), n° 384
7. Cerqueti R., Correani L., Di Dio F. (2016), Optimality and Consistency of Environmental policies in a Differential Game. mimeo
8. Correani L. (2016) A note on Network Stability in a Three-firm Hotelling game. mimeo
9. Correani L., (2016) Networks of collaboration in a three firm Hotelling game. Mimeo
10. Federici A., Garofalo G., Guarini G., L.Manduzio e C.Martini (2015) Efficienza energetica e sviluppo socio-economico, scheda del "27° Rapporto Italia Eurispes", Roma, 2015, pp. 337-350
11. Garofalo G., Pugliesi S., Moschetti A. (2016) Reti d'impresa: una strategia innovativa per l'efficienza energetica. In: ENEA Rapporto annuale sull'efficienza energetica, pp. 91-94
12. Guarini G. (2015) "Complementarity between environmental efficiency and labour productivity in a cumulative growth process", *PSL Quarterly Review*, vol. 68 n. 272, pp. 41-56.
13. Guarini G. Porcile G. (2016) "Sustainability in a post-Keynesian growth model for an open economy", *Ecological Economics*, 126, pp.14-22
14. Guarini G., Fabrizi A., Meliciani V. (2016) "The Effects of Networks and Environmental Policies on Green Patents: an application to the European Countries". mimeo

15. Guarini G., Garofalo G., Federici A. (2016) “Innovative, Inclusive and Eco-Sustainable Growth in Europe: A Structuralist-Keynesian Approach”, *Rivista di politica economica* (in corso di pubblicazione).

Obiettivo d

16. “Welding of automotive aluminium alloys by laser wobbling process” Giuseppe Barbieri, Francesco Cognini, Massimo Moncada, Antonio Rinaldi, ENEA, Gabriele Lapi University of Rome - Tor Vergata, Department of Industrial Engineering, Materials Science & Engineering
17. “IN792 DS superalloy: Optimization of EB welding and post-welding heat treatments”, Giuseppe Barbieri”, Peiman Soltani, Saulius Kaciulis, Roberto Montanari, Alessandra Varone ENEA, Materials by Chemical & Physical Processes
18. “Sviluppo di un sistema (semi)automatico di progettazione di apparecchiature per la conservazione di alimenti attraverso pef”, Paola Casti, M. Salmieri, F. Bonfà, I. Bertini, S. Ferrari, GMEE, Benevento 19-21 settembre 2016.

2 Partecipazione a convegni e a workshop

Obiettivo a

1. Lecture degli esperti ENEA per gli studenti del Corso di Laurea Magistrale in Design di Prodotto Internazionale dell'Università Sapienza di Roma, Sede ENEA, 18 novembre 2015
2. Giornata di formazione continua in collaborazione con l'Ordine dei giornalisti della Lombardia - Le nuove sfide per l'efficienza energetica, fra risparmio sulla bolletta e lotta al cambiamento climatico, Milano, 4 aprile 2016
3. Su specifica richiesta delle Associazioni di categoria italiane ed euripee ENEA ha partecipato a incontri informativi per illustrare i contenuti delle misure di etichettatura ed ecodesign approvate e delle loro ricadute a livello nazionale concentrandosi in particolare sugli aspetti della sorveglianza del mercato. In particolare:
    - Nuovi incentivi e regole per la termica da biomasse, organizzato da AIEL nell'ambito di Progetto Fuoco, Verona, 26 febbraio 2016
    - Workshop Thermo evolution, Da nuove regole a nuove opportunità, MCE 2016, organizzato da ANGAISA, ASSISTAL e ASSOTERMICA, Rho Fiera, 16 marzo 2016
    - C.T. Unicalor organizzato da CECED Italia, Arsiero (Vicenza), 22 aprile 2016
    - Convegno sulla Refrigerazione Professionale, organizzato da CECED Italia e EFCEM Italia, Milano, 6 maggio 2016
    - F-GAS AND ECODESIGN influences of EU legislation on Italian industry, organizzato da EPEE, Mestre (Venezia), 09 maggio 2016
    - International stakeholder meeting, organizzato da ANIMA/Eurovent, Verona, 17 giugno 2016

Obiettivo c

4. Nell' ambito dell'attività per sensibilizzare le imprese sull'importanza di compilare il file riepilogativo contenente i dati aggiuntivi su cui si sono basate le attività relative all'Accordo di Programma Ricerca del sistema elettrico, sono stati effettuati numerosi incontri, con le associazioni di categoria.
   A Roma (presso sede centrale ENEA):
    - 13 Ottobre 2015
    - 22 Dicembre 2015
    - 23 Gennaio 2016
    - 12 Febbraio 2016
    - 7 aprile 2016
    - maggio 2016
    - 16 giugno 2016
    - 16 settembre 2016

   A Milano (varie sedi ospitanti e Assolombarda):
    - 8 ottobre 2015
    - 20 novembre 2015
    - febbraio 2016
    - 22 aprile 2016
    - 24 giugno 2016
    - 21 settembre 2016

   Confindustria altri appuntamenti
    - 22 ottobre 2015 Confindustria Bergamo

- 23 ottobre 2015 AIB Brescia
- 9 novembre 2015 Confindustria Salerno
- 18 novembre 2015AIB Brescia
- febbraio 2016 Confindustria Monza Brianza
- 7 marzo 1016 Assolombarda
- 17 marzo AIB Brescia
- 13 aprile 2016 Assolombarda
- 21 aprile 2016 Confindustria Alessandria
- 28 aprile 2016 Confindustria Bari
- 19 maggio 2016 Confindustria Mantova

Ordine degli Ingegneri

- 14 ottobre2015
- 25 maggio 2016

Altri convegni

- 20 novembre 2015 Centro ENEA di Portici
- dicembre 2015 Certiquality
- 17 febbraio 2016 – 3 marzo 2016 ANIE
- 2 marzo 2016 Regione Emilia Romagna
- 22 marzo 2016 bureau veritas
- 14 aprile 2016 Assoesco
- 19 maggio 2016 Megalia
- 24 maggio industria 4.0
- 8 giugno 2016 Soiel International
- 9 giugno 2016 Consorzio Ponte Rosso San Vito al Tagliamento
- 27 settembre Energy 4.0 Torino
- 29 settembre BIC Lazio a Colleferro

5. Smart energy expo evento sulle diagnosi e angolo di incontro per tre giorni presso lo stand ENEA 14-16 ottobre 2015
6. Rimini key-energy, l'esperto risponde presso lo stand di Assoesco e tre convegni 3-5 novembre 2015
7. ABIlab, 7 ottobre 2015 e 19 novembre 2015
8. GDO, 29 ottobre 2015 Bologna e 30 ottobre 2015Milano
9. Assofond, 16 marzo 2016 e 12-13 maggio 2016
10. Federutility, 15 dicembre 2015
11. Federazione gomma-plastica, 20-21 giugno 2016
12. Assoceramica, 1 giugno 2016 e 6 luglio 2016
13. L'efficienza energetica, una questione di misura Workshop Le nuove sfide per l'efficienza energetica, fra risparmio sulla bolletta e lotta ai cambiamenti climatici, Giornata di formazione continua in collaborazione con l'Ordine dei giornalisti del Lazio, Sede Centrale ENEA - Roma, 6 aprile 2016
14. Energia q.b.: la vera sfida è l'efficienza energetica, Festival Caffeina - E4F: aspetti ingegneristici ed economici. Università ed enti di ricerca a confronto, Viterbo, 28 giugno2016
15. Energy efficiency monitoring in Italy: the 2015 annual report, Workshop Climate change strategies: Contribution of the energy efficiency policies monitoring, Agence Française du Développment (ADF), Parigi, 29-30 Settembre 2015.
16. Il monitoraggio dell'efficienza energetica in Italia, Turkey Study Visit on Energy Efficiency Policies and Measures, Sede Centrale ENEA - Roma, 29 Aprile, 2016

Obiettivo d

17. “Welding of automotive aluminium alloys by laser wobbling process”, Giuseppe Barbieri, Francesco Cognini, Massimo Moncada, Antonio Rinaldi, Gabriele Lapi, Convegno THERMEC’2016 - International Conference on Processing & Manufacturing of advanced Materials Maggio 2016 Graz-Austria (anche in fase di pubblicazione sulla rivista Materials Science & Engineering)
18. “SIN792 DS super alloy: Optimization of EB welding and post-welding heat treatments”, Giuseppe Barbieri, Peiman Soltani, Saulius Kaciulis, Roberto Montanari, Alessandra Varone, Convegno THERMEC’2016 - International Conference on Processing & Manufacturing of advanced Materials May 29 - June 3, 2016 GRAZ, AUSTRIA (anche in fase di pubblicazione sulla rivista Materials Science & Engineering)

3 Appendice

INFORMAZIONE SUI RISULTATI DELL'INDAGINE SULL'ETICHETTA ENERGETICA NEI PUNTI VENDITA (obiettivo a)

18 novembre 2015, Roma

Product Design Studio 4

prof. Loredana Di Lucchio | prof. Michele Capasso
Scientific Support: arch. Antonio Disi, Roberta Moneta (UTEE_ENEA)
Teaching Assistant: Viktor Malakuczi

Nell'ambito della collaborazione che UTEE-SCEE ha attivato con il Corso di Laurea Magistrale in Design di Prodotto Internazionale - Corso Product Design Studio 4 dell'Università La Sapienza di Roma, mercoledì 18 novembre 2015 dalle ore 10.30 alle ore 15.30 presso il salone centrale della Sede ENEA Antonio Disi e Milena Presutto terranno una lecture su Etichettatura energetica ed Ecodesign.

Questa edizione del Corso in Product Design Studio 4 è stata dedicata alle home appliances ed in particolare ai white goods (lavastoviglie, lavatrici, frigoriferi/congelatori).

Le aziende prestano una forte attenzione alla questione dell'efficienza energetica ed alla costante innovazione di questi prodotti, mentre i consumatori sembrano non essere in grado di comprendere tutte le nuove prestazioni. Il risultato è una sorta di disconnessione tra il potenziale di efficienza energetica di questi prodotti e come essi vengono utilizzati nella quotidianità.

Il corso intende fornire una risposta operativa a questo gap. Gli studenti svilupperanno nuovi prodotti/servizi che consentano alle persone di avere un uso più efficiente degli elettrodomestici in casa, al fine di ottenere comportamenti più sostenibili.

AGENDA

ore 10.00 **Registrazione partecipanti**

ore 10.30 **Introduzione** - ***Antonio Disi***

ore 11.00 **Ecodesign ed Etichettatura energetica** - ***Milena Presutto***

ore 13.00 **Pausa pranzo**

ore 14.00 **Q&A** – ***Milena Presutto***

ore 16.00 **Conclusione**

Ecodesign ed etichettatura energetica: una lecture degli esperti ENEA per gli student... Pagina 1 di 1

Agenzia Nazionale Efficienza Energetica

ENEA

Ecodesign ed etichettatura energetica: una lecture degli esperti ENEA per gli studenti del Corso di Laurea Magistrale in Design di Prodotto Internazionale dell'Università Sapienza di Roma

Agenzia Nazionale per l'Efficienza Energetica-ENEA


dr. Milena Presutto - UTEE
Ecodesign, energy labelling,
green public procurement,
consumer behaviour,
market surveillance,
design for accessibility,
circular economy,
standards,
.....
Corso in Product Design Studio 4, 18 November 2015

04 aprile 2016, Milano

DIFFUSIONE DELL' INFORMAZIONE SULLA SORVEGLIANZA DEL MERCATO

26 febbraio 2016, Verona

16 marzo 2016, Rho Fiera

22 aprile 2016, Arsiero (Vicenza)

Subject: CT Unicalor - 22 Aprile 2016 Ore 10:30 - ODG

Content-Type: multipart/related;

MIME-Version: 1.0

Davide Castagna

Senior Key Account Manager

CONFINDUSTRIA CECED ITALIA

06 maggio 2016

ceced Italia

EFCEM ITALIA

CONVEGNO REFRIGERAZIONE PROFESSIONALE

Milano, 6 maggio 2016

Presso IMQ

Via Quintiliano, 43 – Milano

Il Convegno è dedicato ai temi dell'*Energy Labelling*, dell'*Ecodesign* e della *Sorveglianza di Mercato* in recepimento dei *Regolamenti 1094-1095/2015*, curandone gli aspetti più rilevanti per la loro applicazione.

Programma della giornata:

10.00 – Accredito partecipanti	
10.15 – Apertura Lavori, presentazione Efcem Italia	Mara Rossi (CECED ITALIA)
10.30 – Reg. 1094-1095/2015: Obblighi operatori economici	Mara Rossi (CECED ITALIA)
10.45 – Reg. 1094-1095/2015: Requisiti applicativi	Fabio Gargantini (CECED ITALIA)
11.15 – Applicazione norma EN 16825	Roberto Clini (IMQ)
11.40 – Coffee break	
12.00 – Verifica della conformità per i prodotti professionali	Milena Presutto (ENEA)
12.30 – Promozione dei prodotti efficienti	Luca Galeasso (INNOCAT) Andrea Roscetti (PROCOLD)
13.00 – *Question time*	
13.30 – Chiusura lavori	

Si prega di confermare la propria partecipazione scrivendo a segreteria@cecedItalia.it **entro e non oltre mercoledì 27 aprile**, la disponibilità è garantita fino ad esaurimento posti. Il convegno è aperto **agli associati CECED Italia e ai non associati, per questi ultimi la quota di adesione è di euro 350 + iva**, cifra che sarà tenuta a titolo di acconto per le aziende che aderiranno a CECED Italia entro il 2016.

Gruppo Efcem Italia si posiziona quale unico rappresentante italiano nell'Associazione europea Efcem, delegata a rappresentare il comparto. Gruppo Efcem Italia nasce da Ceced Italia, l'Associazione confindustriale delle aziende di apparecchi domestici e professionali in Italia. Il comparto italiano delle apparecchiature professionali per il catering equipment è leader nel mondo per qualità e livello di servizio. Le aziende rappresentate da Efcem Italia hanno fatturato nel 2015 circa € 2,8 miliardi. L'export varia dal 40 all'80% a seconda della tipologie di prodotto.


Convegno refrigerazione professionale
CECED Italia/EFCEM Italia
ENEA
Verifica della conformità:
i prodotti professionali
dr.ssa Milena Presutto
UTEE - Unità Tecnica Efficienza Energetica
6 maggio 2016, Milano
www.efficienzaenergetica.enea.it

09 maggio 2016, Mestre (Venezia)

17 giugno 2016, Verona

INFORMAZIONE SUI RISULTATI DELL'INDAGINE SULL'ETICHETTA ENERGETICA NEI PUNTI VENDITA

05 ottobre 2016, Milano

CAMERA DI COMMERCIO MILANO

ENEA

L'ETICHETTA ENERGETICA NEI PUNTI VENDITA LUCI ED OMBRE
Indagine mercato 2016

Mercoledì, 5 ottobre 2016
ore 09.30
Palazzo Giureconsulti - Sala Esposizioni
Milano, Via Mercanti, 2

Programma

Iscriviti online!

Raccolta articoli

Renewable Energy xxx (2016) 1–10

Contents lists available at ScienceDirect

Renewable Energy

journal homepage: www.elsevier.com/locate/renene

Nanostructured metal hydride – Polymer composite as fixed bed for sorption technologies. Advantages of an innovative combined approach by high-energy ball milling and extrusion techniques

Marzia Pentimalli [a, *], Enrico Imperi [b], Alessandro Zaccagnini [b, c], Franco Padella [a]

[a] ENEA – Italian National Agency for Energy, New Technologies and Sustainable Economic Development, Casaccia Research Centre, Via Anguillarese 301, 00123 Rome, Italy
[b] LABOR s.r.l. – Industrial Research Laboratory, Via Giacomo Peroni 386, 00131 Rome, Italy
[c] Department of Industrial Engineering, University of Rome Tor Vergata, Via del Politecnico 1, 00133 Rome, Italy

ARTICLE INFO

Article history:
Received 23 May 2016
Received in revised form
26 July 2016
Accepted 29 July 2016
Available online xxx

Keywords:
Metal hydride
Polymeric matrix
Extrusion
Ball milling
Sorption
Heat pump
Waste heat recovery

ABSTRACT

Different metal alloys can react highly exothermically and reversibly with hydrogen to form metal hydrides. Based on these reactions several application have been developed, e.g. in fuel cell, in storage for hydrogen gas and in sorption heat pumps. By exploiting the thermodynamical properties of some metal hydriding alloys, cooling energy can be generated by using renewable, sustainable and/or disposable energy sources. However, hydriding alloys show some limitations in their behaviour mainly regarding their intrinsic low thermal conductivity and mechanical stability during the hydriding process. A proper management of these issues is required in practical applications in particular when the metal hydrides have to be stably packed as fixed beds with good mechanical stability, high thermal conductivity, fast kinetics, reproducibility, durability.

In this work a composite material containing a high metal fraction is obtained by an innovative bulk and low cost processing approach by combining high-energy ball milling and extrusion techniques. The methodology is presented and the characterization of a representative $LaNi_5$-type based composite is given. The developed composites were used as fixed beds in the implementation of a Metal Hydride Cooling System. Finally, the system was integrated into a refrigerated transportation vehicle, currently under testing. Some results are reported coming from a preliminary test campaign.

1. Introduction

Every metal hydride-based device should contain the hydriding metals in form of powder to increase the active surface. Also, the repeated hydrogen loading–unloading cycles induce further pulverization of the metal particles due to the large volume mismatch between the hydride and the metal phases [1,2]. Management of free metal powder in fixed beds is required, avoiding the negative effects possibly deriving by powder material transportation due to the hydrogen flux throughout the beds.

Moreover, as the chemical interaction of hydrogen with a metal involves heat exchanges (metal hydride formation is exothermic and H_2 release from the metal-hydrogen compound is endothermic), a proper heat management throughout the material's bed is also required to optimize the thermal conductivity of the material so that heat enters and leaves the material as quickly as possible with beneficial effects in maintaining high adsorption/desorption rates. Besides to the possibility of a proper designing of the fixed beds (for example by adding fins that help with heat transfer), various techniques have been proposed to improve the overall material mechanical stability and thermal conductivity such as compaction of porous metallic matrix, microencapsulated metal hydride compacts, insertion of aluminium foam, integration of copper wire nets, and so on [3–9].

We previously demonstrated [10,11] that the physical–chemical characteristics of Acrylonitrile Butadiene Styrene (ABS) copolymer results suitable for using as embedding matrix for hydrogen storage materials. In facts, in comparison with other well-crystallized polymeric material, the ABS does not show significant gas barrier behaviour, the diffusion processes being favoured by the disordered physical conformation of its polymeric chains. In addition, the presence of the rubber component is able to easily compensate the

* Corresponding author.
E-mail address: marzia.pentimalli@enea.it (M. Pentimalli).

http://dx.doi.org/10.1016/j.renene.2016.07.074
0960-1481/

volumetric variations exhibited by the alloy phase during H_2 loading and unloading cycling inside the embedding polymeric matrix.

We also reported [12,13] about the possibility of enhancing the overall thermal conductivity of metal hydrides embedded in a silica matrix by the addition of an amount of conductive filler. It was assessed that: i) the method of loading the matrix with a conductive filler is suitable to enhance the overall thermal conductivity; ii) the filler in form of graphite powder results much efficient with respect to the flakes; iii) the addition of 10% V of filler is sufficient to obtain an increase of one order of magnitude of the thermal conductivity of the composite with respect of the value of the starting metal hydride (typically for $LaNi_5$, $\lambda \approx 0.1$ W/mK) with minimal expected structural modification with respect to a reference sample.

Clearly, the use of a unique and simple material processing approach to address both the issues of powder dispersion risks and low thermal conductivity would result practically advantageous. In addition, when considerable amounts of active metal phases are required for implementing practical devices, the material processing has to necessarily be based on low cost and easily scalable techniques.

Here, at the aim to develop a metal hydride-matrix composite able to embed the hydriding particles with minimal detrimental effects on the end performances and having enhanced thermal conductivity, we propose an innovative material processing approach based on a combination of ball milling and extrusion techniques.

Based on the previous experience, the ABS copolymer is chosen as matrix also due to its rheological and thermal properties that make it easily workable by extrusion and, not last, for its wide availability and low cost. Due to the extremely challenging required composition for the final composite material (low polymer content), an accurate tuning of the processing technologies was necessary and crucial mainly to overcome the homogeneity concerns deriving from the enormous difference in the densities of the polymeric matrix (about 1 g/cm^3), the graphitic filler (about 2 g/cm^3) and the metal alloy (more than 8 g/cm^3) counterparts, respectively.

In this work we used various AB5 particles alloys as active materials to be embedded in an ABS matrix containing graphite powder as filler. The chemical-physical and functional characterizations of the obtained composite samples are reported.

Some of the developed composites were used as active materials assembled in fixed beds to implement an innovative metal hydride-based heat pump system. Some preliminary results as obtained from the testing of the heat pump system are also related about.

2. Materials and methods

2.1. The metal hydride

In this work we used different $LaNi_5$-type metal hydride alloys (particles size 1 ÷ 100 μm diameter) supplied by Saes Getters. The alloys were preliminarily tested to check their stability with respect the mechanical action in air. For the purpose some portions were milling treated in a stainless steel cylindrical vial (60 cm^3 volume) by means of a SPEX 8000 M High Energy Miller apparatus. Samples aliquots were milled with stainless steel balls (10 mm diameter) with a constant powder to balls ratio of 1:10 (typically, 4 g of alloy and 40 g of milling media). Samples were prepared at 15, 30, 60, 90 and 120 min milling times, respectively. The metal samples to be used as particulate dispersion into the composite were directly obtained in the Zoz Simoloyer CM02, preliminarily to the successive blending action (see in the following), by milling about 1 kg of the starting at 1000 rpm for 10 min (2 L vial, stainless steel balls, 5 mm diameter, about 1:12 powder to balls ratio).

2.2. The polymeric matrix

The ABS Sinkral® used in this work as embedding matrix was supplied by Versalis Spa coming from an industrial production process of mass polymerization. The resulting polymer shows good strength, toughness, impact resistance and dimensional stability properties. Samples were supplied in form of spherical pellets and reduced in powder particles by using centrifugal milling technique (Fritsch Pulverizette 14 high-speed rotor mill) after their embrittlement in liquid nitrogen. The centrifugal action was carried out at 15000 rpm with a 0.5 mm diameter sieve.

2.3. The conductive filler

A low cost commercial graphite powder (99% purity, <2 mm particle diameter, ≈2 €/kg Aldrich) was used as conductive filler of the polymeric matrix. A loading amount of 10% in volume of fresh, as received, graphite powder was added to the metal phase and blended by means of the high-energy ball milling treatment described here below.

2.4. Blending of the metal-matrix-filler mixture by ball milling

The metal-matrix-filler mixtures containing the three components in 45/45/10 vol ratios were blended by means of high-energy ball milling using a Zoz Simoloyer CM02 apparatus. The vial (2 L volume) was filled with the material and the milling media (stainless steel balls, 5 mm diameter) with a constant powder to balls ratio of 1:10. The treatment consisted in a preliminary milling (15 min at 1000 rpm) of the metal alloy-graphite mixture followed by a successive milling for (5 min at 1000 rpm) after the addition of the polymeric fraction. At the end the blended batch (about 1.2 kg) was recovered from the vial and separated from the ball media trough a 3 mm diameter sieve.

2.5. Extrusion of the metal-matrix-filler blend

The metal-matrix-filler blends as obtained by the above described ball milling treatment were extruded by using a bench top Compounder ZK 25T x 18/24 D by Dr. Collin GmbH. The apparatus is equipped with two counter-rotating twin screws, a volumetric feeding system, an in-line water bath to cool the extruded wire followed by a pelletizer to reduce the wire in cylindrical pellets. The process was carried on at 67 rpm tween screws speed. The thermal profile of the apparatus was set at 110/130/150/200/220 °C for the five zones, respectively. The final composite was obtained in form of wire and cut in form of cylindrical pellets (≈2 mm diameter per ≈3 mm height) by means of the pelletizer.

2.6. Chemical physical and functional characterization

X-ray diffraction analyses were carried on the $LaNi_5$-type alloy for the as received, milled and final composite samples. The diffraction patterns were obtained by using a X-RED 3000 instrument by Italstructure equipped with a Fe emitting tube, monochromator on the primary beam and a simultaneous INEL detector with 4097 channels corresponding to 120° of simultaneous data acquisition. Comparing the experimental data with the standard cards of the JCPDS-ICDD 1999 database phase identification was assessed.

The *morphological features* of the samples were observed by high resolution scanning electron microscopy analyses using a FE-SEM LEO 1530 microscope.

Please cite this article in press as: M. Pentimalli, et al., Nanostructured metal hydride – Polymer composite as fixed bed for sorption technologies. Advantages of an innovative combined approach by high-energy ball milling and extrusion techniques, Renewable Energy (2016), http://dx.doi.org/10.1016/j.renene.2016.07.074

Thermal conductivity measurements were conducted by using the commercial analyser Mathis TCi by Setaram. The operating principle of the instrument is based on the modified transient plane source: a sensor applies a momentary heat source to the sample. This causes a slight temperature rise at the sensor-sample interface, inducing a change in the voltage drop of the sensor element. Since the rate of temperature rise at the heating element is proportional to the thermal conductivity of the material, this property can be determined by measuring the rate of voltage rise when a constant current is applied. The instrument allows measurements in the range of thermal conductivity from 0 to 100 W/(mK), temperature from −50 to 200 °C, with a precision better than 1% and an accuracy about 10%. The duration of each measurement was about 45 s.

Attenuated Total Reflection infrared spectra (ATR) were recorded on a Nicolet FT-IR (ThermoElectron C0. Madison, WI, USA) equipped with a Golden Gate diamond single reflection device (Specac).

The hydriding behaviour of the alloys was studied by both the *Pressure Differential Scanning Calorimetry (PDSC)* non-equilibrium method and by the equilibrium isothermal *Pressure Composition Temperature (PCT)* method.

The calorimetric measurements were carried on by using a Perkin Elmer DSC7 apparatus equipped with a high-pressure cell (Perkin Elmer), two gas pressure controllers (Bronkhorst) and a mass flow controller (Bronkhorst). The experimental set-up is shown elsewhere [10]. The calorimeter head, pressurized up to 30 atm, operates in the 25–600 °C temperature range. The sample enclosure block sealing is guaranteed by the use of a high-pressure cell cover. The enclosure block is equipped with built-in connections allowing a liquid cooling system to be integrated inside the block.

Before each experiment the samples were kept under vacuum at 200 °C for 20 min to eliminate contaminants. This was followed by an activation stage of the metal phase performed at constant H_2 pressure (30 atm) by heating the material up until a clear evidence of thermal phenomena (due to the interaction with hydrogen) is shown.

The PCT equilibrium isotherm diagram of the alloy was obtained by using the Sievert volumetric method: the amount of absorbed gas was calculated by analysing the pressure drop of H_2 gas in equilibrium with the partially hydrided material at constant temperature in a volume-calibrated system. The experimental determinations of the amount of absorbed hydrogen were preceded by a calibration phase, which was repeated for all the different temperatures of analysis. The volumes were mathematically corrected by taking into account the volume occupied by the sample as estimated by measuring its mass and density. The analysed samples were subjected to a preparation procedure consisting in two successive steps namely purging and activation. The purging phase (to remove the contaminants eventually present on the sample), consisted in cycling the sample under H_2 gas pressure (10^{-2}–5 atm) at 100 °C. The activation procedure consisted in temperature cycling the sample under hydrogen atmosphere (30 atm). The effectiveness of the activation was assessed by pressure measurements and evaluating the resulting pressure drops. At the end the sample was further evacuated for 1 h before the effective isotherms acquiring. Each measurement consisted in repeated acquisitions of the equilibrium pressures operated in the 0–30 atm H_2 pressure range at defined temperature values. For this, the experimental acquisition time is intrinsically strongly dependent from the nature of the measured sample.

3. Results and discussion

The material processing approach here presented is based on a combination of high-energy ball milling and extrusion techniques. After a preliminary check on the alloy resistance to mechanical treatments, the material processing consisted in the following main steps: 1) powdering of the polymeric material; 2) ball milling of the hydriding alloy and blending of all components and 3) extrusion of the blend and production of the metal hydride – polymer composite in form of pellets. Various chemical-physical and functional characterizations were carried out during the successive phases.

3.1. Metal alloys treatment by high-energy ball milling

Evaluation of the milling action on the AB5 type alloy. One of the steps of the material processing requires the treatment of the metal to obtain nanostructured alloy. In facts the gas-solid reaction exhibits rates that are strongly dependant by the surface area exposed to the reactive gas. Moreover in the presence of diffusion phenomena, such as for H_2 inside the metal, a high concentration of defects in the bulk material greatly favours the reaction kinetics. Thus, at the aim of both enhancing the extent of the accessible surfaces and the concentration of defects, the metal alloys undergone a high-energy ball milling treatment. To check the effect of the mechanical action to the milled alloy in standard environmental atmosphere, a preliminary test was conducted in the Spex 8000 Miller. In Fig. 1 the X-ray diffraction patterns of the $LaNi_5$-type alloy milled at different milling time are reported as a function of the milling time. The milling action produces a broadening of the diffraction profile after few minutes of processing. At 60 min partial peak overlapping is observed with consequent loss of the individual signals characteristics. Starting from 90 min milling time the system exhibits a remarkable broadening and few overlapped signals below $2\Theta = 70°$ are detectable. At 120 min a new well defined peak at $2\Theta = 57°$ is clearly shown. Actually some traces can be evidenced after 60 min milling (evidenced by * in the figure). By comparing the XRD profile with the card JCPDS n. 4–850 the new peak can be assigned to the main peak of metallic Nickel. This indicates that, starting from 1 h of treatment in air, the repeated milling action is able to produce a demixing of the alloy probably due to the formation of amorphous Lanthanum oxide La_2O_3.

In Fig. 2 the alloy grain size values as obtained by applying the Sherrer Formula on the main peak deconvoluted from the

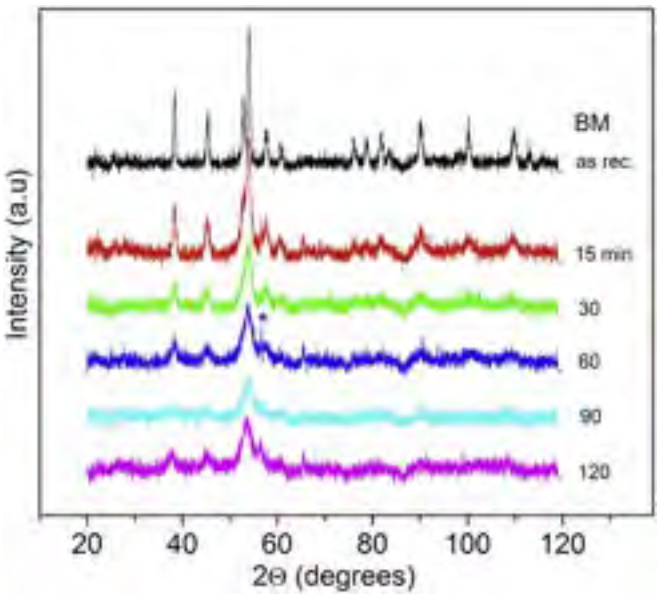

Fig. 1. X-ray diffraction pattern sequence of $LaNi_5$–type alloy as a function of different milling times.

Please cite this article in press as: M. Pentimalli, et al., Nanostructured metal hydride – Polymer composite as fixed bed for sorption technologies. Advantages of an innovative combined approach by high-energy ball milling and extrusion techniques, Renewable Energy (2016), http://dx.doi.org/10.1016/j.renene.2016.07.074

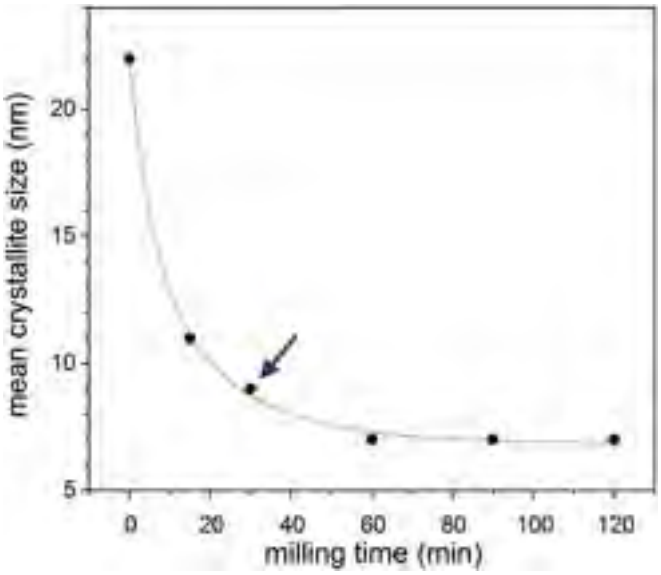

Fig. 2. Crystallite size of the system $LaNi_5$–type at different milling times.

broadening effects of the other peaks, are plotted versus the time of treatment. Starting form crystalline domains of about 20 nm the $LaNi_5$-type grain size results decreased down to 10 nm after 15 min of treatment and remains constant at about 7 nm after 60 min milling. At 30 min, while the de-mixing phenomena are not still detectable, the mean crystallite size is quite constantly about 8–9 nm. Thus, the milling time of 30 min resulted sufficient to reduce the grain size below 10 nm domains and contemporary avoiding undesired degradation phenomena. On this basis the overall mechanical treatment do not overcome a total time of 30 min.

The SEM image of the $LaNi_5$-type sample as received is reported in Fig. 3A. The powder is constituted by particles with size between 1 and 50 ÷ 100 μm with irregular shape. After 30 min of milling the compact aspect exhibited by the samples as received has changed in agglomerates of nanometre-sized porous sub structures (see Fig. 3B). The presence of microstructures and cavities at the nanometre scale is also evident in the in the inset of Fig. 3B. The milling process produces a nanometre-sized structured powder that exhibits a porous surface.

1) The first step of the process consists in the treatment of the ABS to reduce the polymer from the received pellet form into powder. The centrifugal high-speed rotor mill is utilised. The titanium rotor is set in the rotation mode at 15000 rpm and accelerates the polymer pellets against the sieve's walls. After embrittlement in liquid nitrogen, the operator uploads the cold pellets into the hopper of the instrument and the powder is directly collected into a tissue bag. This treatment in lab scale mill allows obtaining about 250 g per hours of polymer powder with 1 mm equivalent particles diameter. In Fig. 4 two images are shown relative to the polymer in pellet and powder forms, before and after the centrifugal milling, respectively.

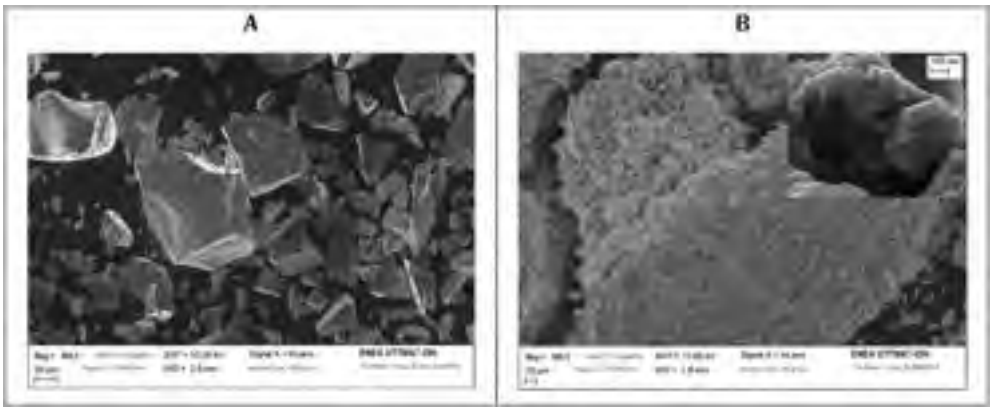

Fig. 3. Scanning Electron Microscopy images of $LaNi_5$-type alloy as received (A) and milled for 30 min (B).

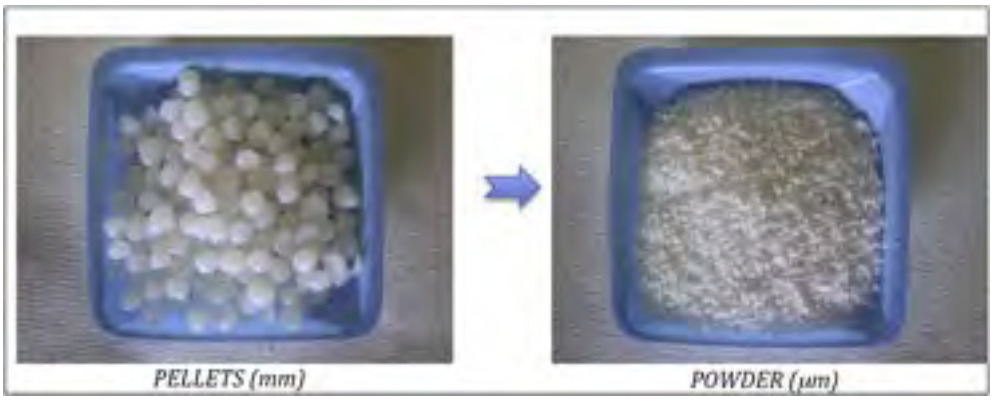

Fig. 4. The Acrylonitrile Butadiene Styrene copolymer in form of commercial pellets and as reduced in powder by means of centrifugal milling after material embrittlement in liquid nitrogen.

Please cite this article in press as: M. Pentimalli, et al., Nanostructured metal hydride – Polymer composite as fixed bed for sorption technologies. Advantages of an innovative combined approach by high-energy ball milling and extrusion techniques, Renewable Energy (2016), http://dx.doi.org/10.1016/j.renene.2016.07.074

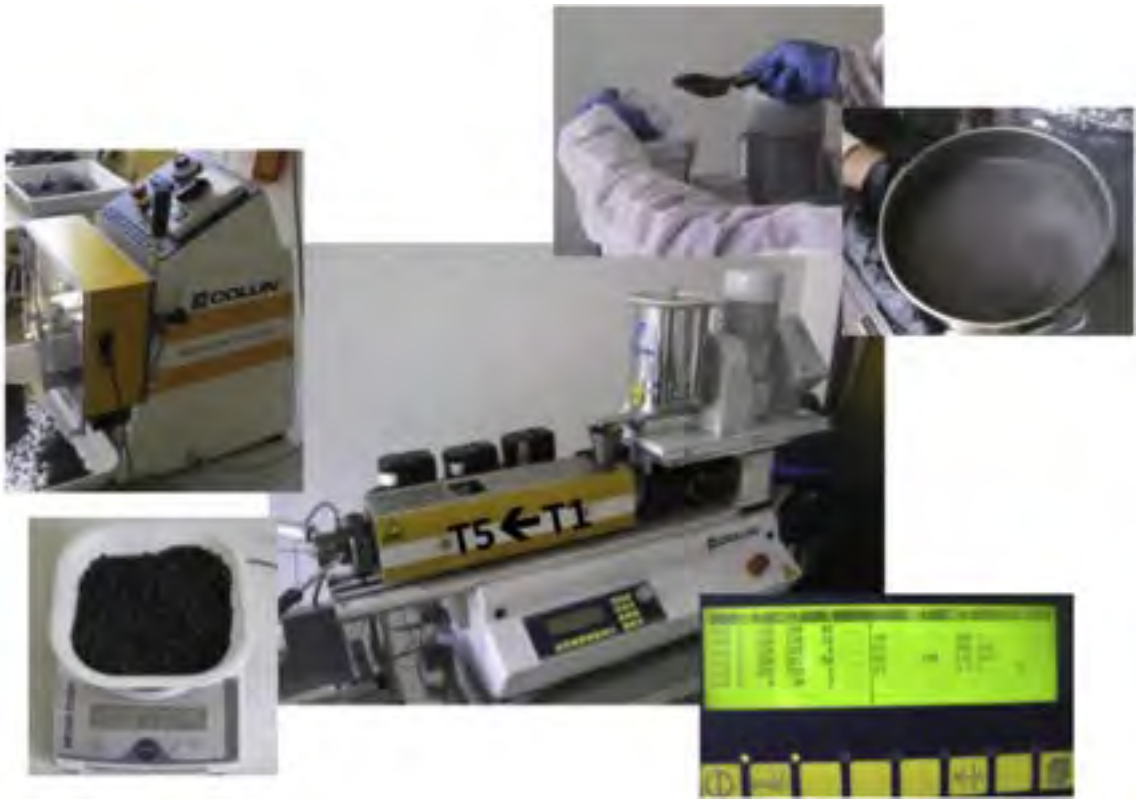

Fig. 5. Twin screw Collin ZK25TSCR15 extruder utilised to obtain the metal hydride - polymer composite. In the wright up side the metal-matrix-filler blend obtained by ball milling is loaded into the dosing unit; the blend is extruded through the successive thermal zones: in the right bottom side the T1-T5 temperature settings are shown on the control panel; the extruded composite at the output is water down cooled and reduced in pellets by means of the in-line pelletizer (left side).

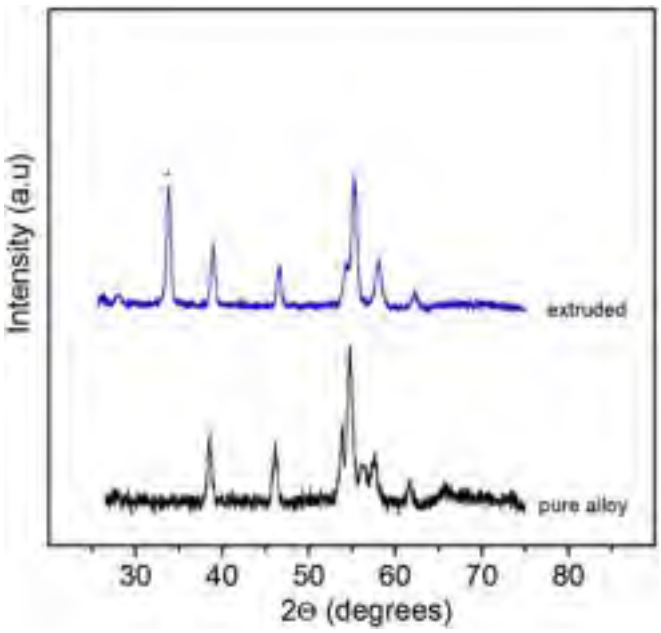

Fig. 6. X-ray diffraction patterns of the extruded metal hydride-polymer composite and the pristine pure $LaNi_5$–type metal hydride.

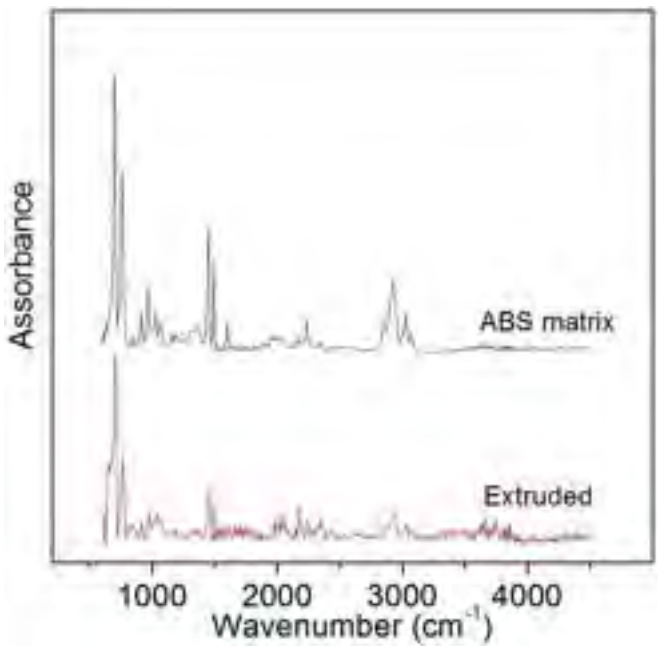

Fig. 7. Comparison of infrared spectra obtained in ATR mode of the extruded composite and pure ABS copolymer. The signals are typical from ABS and can be respectively assigned to: 650-800 cm^{-1} C–H aromatic bending out plane; 730-665 cm^{-1} C–H bending alkene; 1000-1300 cm^{-1} C–H aromatic bending out plane; 1400-1600 cm^{-1} C–C aromatic ring stretching; 1661 cm^{-1} C=C stretching alkene; 2230 cm^{-1} stretching nitrile; 2300 cm^{-1} CO_2 asymmetric stretching; 2300-2900 cm^{-1} C–H stretching of the alkene; 3000-3100 cm^{-1} C–H aromatic stretching.

2) The second phase of the process is the preparation of the metal-matrix-filler blend at high metal content (up to 85% weight of metal; metal/matrix/filler 45/45/10 v/v). Different batches of blended powder of about 1.2 kg were obtained. The single batch

Please cite this article in press as: M. Pentimalli, et al., Nanostructured metal hydride – Polymer composite as fixed bed for sorption technologies. Advantages of an innovative combined approach by high-energy ball milling and extrusion techniques, Renewable Energy (2016), http://dx.doi.org/10.1016/j.renene.2016.07.074

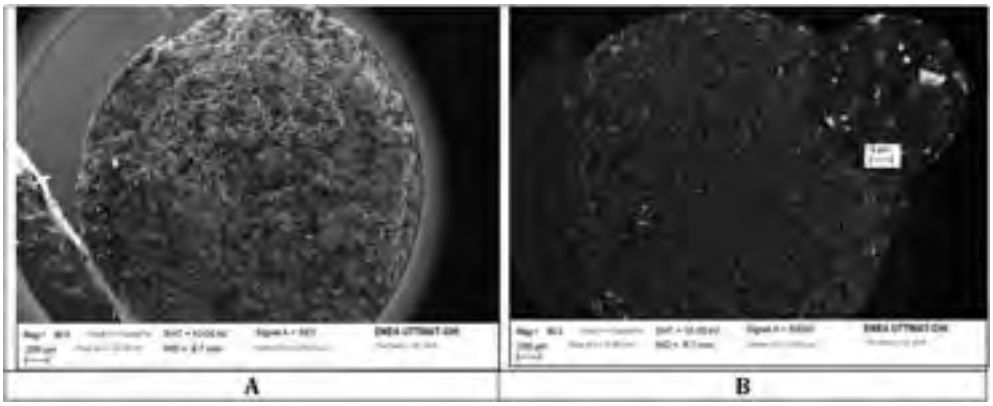

Fig. 8. Scanning Electron Microscopy analyses of the extruded metal hydride-polymer composite. The images refer to transversal sections of the extruded cylindrical pellets.

treatment consists in loading and milling (1000 rpm, 10 min) about 1 kg of metal alloy in the ZOZ CM02 apparatus. Successively the graphite fraction is loaded into the vial and the mixture is milled again at 1000 rpm for 5 min so that further metal nanostructuring and simultaneous compounding with graphite are obtained. Then the polymeric fraction is added and the mixture is milled again at 1000 rpm for 10 min. At the end the whole batch is recovered from the vial and separated from the ball media trough a 3 mm diameter sieve. The final blend results very homogeneous upon observation confirming that the milling treatment is able to homogenise the 3 components by avoiding any segregation due to the differences in material densities. The so obtained metal-matrix-graphite blend is then loaded into the hopper and extruded.

3) In Fig. 5 pictures taken during the last step of the process that consists in applying the extrusion technology at the aim to obtain the final metal hydride-polymer composite are shown. The metal-matrix-graphite blend obtained by the previous step 2) is loaded into an automatic dosing unit set at the minimal rate. Successively, the material is dosed into the extruder, with the following operative conditions: the twin screws speed is set at 67 rpm and the thermal profile of the apparatus is fixed at 110/130/150/200/220 °C for the T1-T5 zones of the extruder, respectively. The melt extruded spaghetti-like composite coming from the output of the apparatus is water-cooled and then reduced in form of cylindrical pellets by means of the in-line pelletizer.

Here in the following the physical-chemical and functional characterizations performed on the metal hydride - polymer composite as obtained by a combination of high-energy ball milling and extrusion techniques, are reported.

In Fig. 6 the X-ray diffraction pattern of the extruded composite is reported in comparison with that coming from the pristine pure $LaNi_5$-type alloy. As expected the only crystalline phases are evidenced from XRD data, being the ABS component in amorphous form. A comparison check of the patterns with JCPDS cards of oxidised metal components permits to exclude oxidative evolution

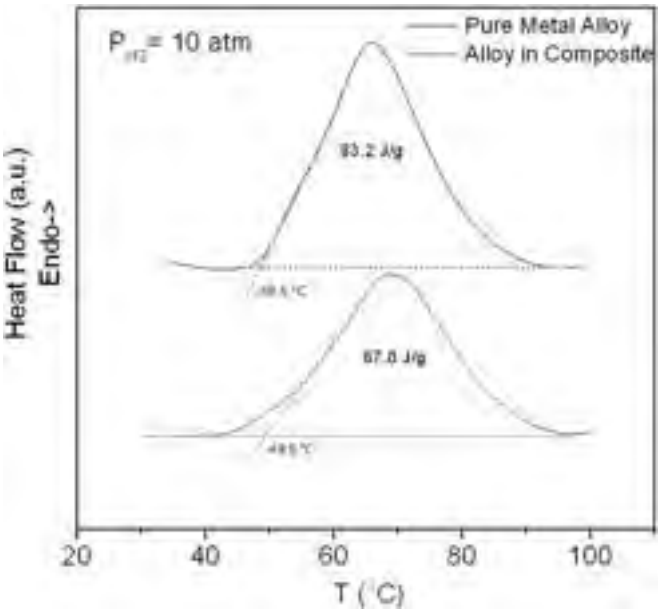

Fig. 9. Differential Scanning Calorimetry traces of obtained at 10 atm H_2 pressure for the extruded metal hydride-polymer composite in comparison with that one obtained for the pristine pure $LaNi_5$–type metal hydride. Data are relative to the dehydriding process.

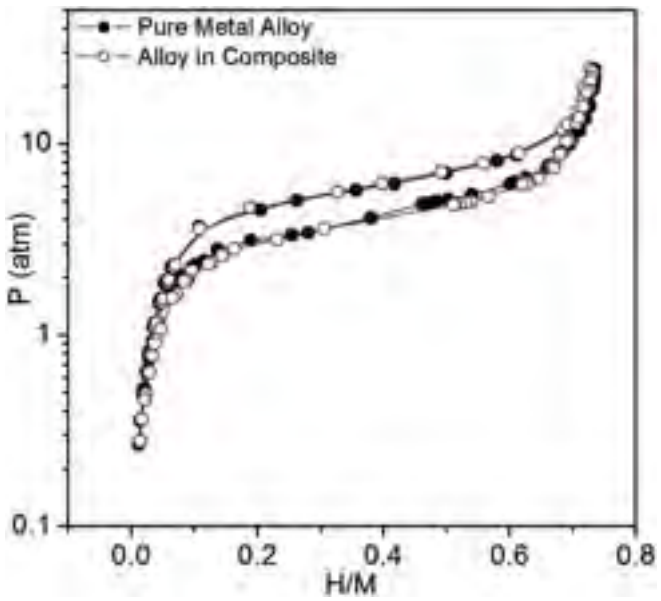

Fig. 10. Normalised Pressure Composition Temperature isotherms obtained at 40 °C for the extruded metal hydride-polymer composite in comparison with that for the pristine pure $LaNi_5$–type metal hydride. Data are relative to a complete hydriding/dehydriding cycle.

Please cite this article in press as: M. Pentimalli, et al., Nanostructured metal hydride – Polymer composite as fixed bed for sorption technologies. Advantages of an innovative combined approach by high-energy ball milling and extrusion techniques, Renewable Energy (2016), http://dx.doi.org/10.1016/j.renene.2016.07.074

of the alloy due to the process. Graphite component is revealed form the only peak falling at about 33.3 2Θ degrees, corresponding to the (001) planes reflex.

In Fig. 7 the infrared analysis of pure ABS clearly shows characteristic absorbance features of the acrylonitrile – butadiene–-styrene copolymer (see the caption). In the same figure the IR spectrum of the extruded composite results quite similar.

Scanning microscopy analysis of a transversal section of extruded composite is reported in Fig. 8. The composite shows an almost homogeneous porous microstructure in the whole section (A). This feature appears to be favourable in terms of gas permeation under hydrogen pressure. The backscattered electrons image (B) shows the distribution of the metal powder particles (white in the image). The metal appears quite homogeneously distributed within the matrix. As evidenced in the magnification reported in the inset, metal particles appear completely embedded in the matrix.

Thermal conductivity measurements were carried on at room temperature by using a modified transient plane source method. The thermal conductivity λ value for the ABS polymer in powder form is found to be equal to 0.22 W/mK (nominal value from technical data sheet, 0.17 W/mK). The λ value measured for the final

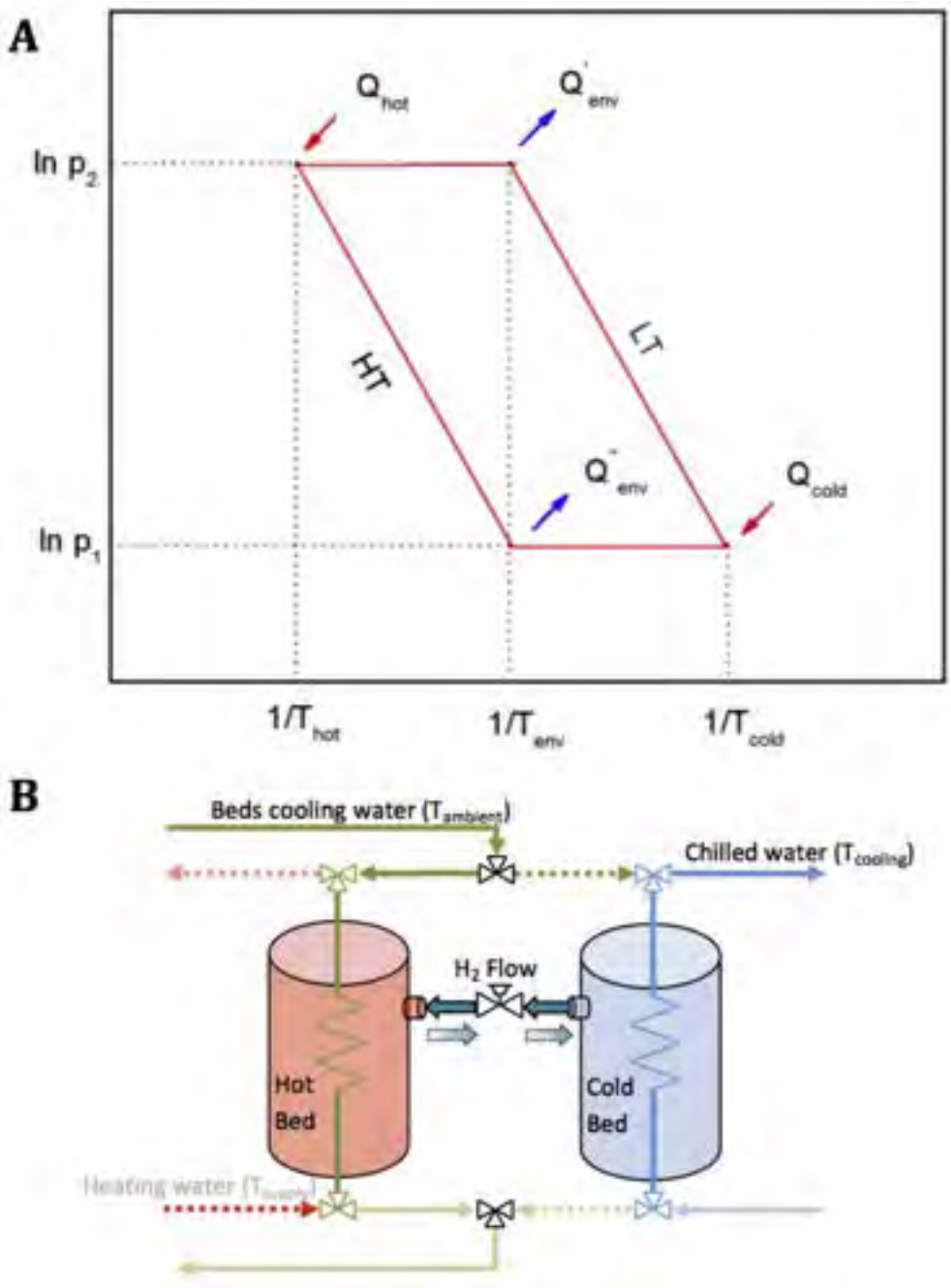

Fig. 11. (A) Schematic thermodynamic cycle of the single stage/single effect configuration as represented in the van't Hoff plane; (B) Conceptual layout of a single stage MHCS in cooling mode. The system comprises a pair of reactors, the hot bed (HB) containing a high temperature hydride (HT) and the cold bed (CB) containing a low temperature hydride (LT). Two energy streams are fed to the cycle, one at high temperature (Q_{hot} at T_{hot}, coming from the source heat that is at $T_{supply} \geq T_{hot}$), and one at low temperature (Q_{cold} at T_{cold}, which is the energy stream removed from the area to be cooled down at $T_{refr} \geq T_{cold}$). Removed heat is expelled toward the external environment, characterized by the third thermal level, T_{env}.

Please cite this article in press as: M. Pentimalli, et al., Nanostructured metal hydride – Polymer composite as fixed bed for sorption technologies. Advantages of an innovative combined approach by high-energy ball milling and extrusion techniques, Renewable Energy (2016), http://dx.doi.org/10.1016/j.renene.2016.07.074

composite is about 2.0 W/mK. This value constitutes a substantial enhancement of the material characteristic when compared to the effective typical values of λ in packed beds of particles (λ ≈ 0.1 W/mK for La-based metal hydride powders). In a general way, the gas pressure plays a very important role in the heat transfer within a fixed bed. In the case of hydriding materials the function of hydrogen gas is particularly relevant in the 1–100 atm range of pressure when the transition between molecular and continuum gas transport within the void spaces occurs. To achieve an equivalent behaviour to the one exhibited by our composite, at least 20 atm of hydrogen gas pressure would be needed for a packed bed of particles [14]. Actually, the λ value obtained for the composite is intrinsically quite high (i.e. not comprising the gas contribution to the heat transportation). Thus, the material results effective to ensure the required heat transfer also during the phases of a thermal cycle operating at low pressure. This produces a favourable condition to use the composite in developing the heat pump sorption-based technology.

In Fig. 9 the DSC characterization of the extruded pellet during its de-hydriding process is reported, in comparison with the pure metal alloy. The alloy inclusion in the matrix leads to just a minimal increase of the onset temperature (i.e. the starting temperature of the de-hydriding process). The entity of the observed temperature shift is irrelevant from the here-proposed technological point of view. As expected, the de-hydriding enthalpy of the composite results about 80% of the pure alloy. This confirms the absence of metal oxide contaminations, due to the protection action probably accomplished by the polymer during the extrusion process.

At the aim to check the composite material behaviour under hydriding/de-hydriding cycling, repeated PCT analyses (10 cycles) are carried on at 40 °C. The analysed sample is obtained by sintering the metal hydride - polymer composite pellets at 170 °C (hot pressing) up to obtain a low relative density of 0.5. In Fig. 10 the resulting isotherms of the sample after its thermal activation and 5 cycles are shown (data are normalised on the metal content). Characteristic curves obtained from the pure metal alloy are also reported. The comparison shows an almost perfect coincidence between the composite and the pure $LaNi_5$-type alloy, confirming the transparency of the polymeric matrix with respect to the hydrogen gas.

3.2. Application of the metal hydride – polymer composite in a heat pump system

Refrigeration systems are widely used in many applications such as air conditioning, food industries, cold storage and others. The use

Fig. 12. Picture views of the vehicle with the assembled Metal Hydride Cooling System prototype (top). In the bottom an image of the insulated refrigerated van with its internal heat exchanger is shown.

Please cite this article in press as: M. Pentimalli, et al., Nanostructured metal hydride – Polymer composite as fixed bed for sorption technologies. Advantages of an innovative combined approach by high-energy ball milling and extrusion techniques, Renewable Energy (2016), http://dx.doi.org/10.1016/j.renene.2016.07.074

of sorption cooling technologies for automotive applications has attracted significant research work as the engine waste heat can drive the systems with beneficial effects on fuel consumption. A number of studies have been carried out since the early nineties and prototypes have been constructed and tested with silica gel/water [15–17], zeolite/water [18–21], activated carbon/ammonia [22,23] and metal hydrides/hydrogen [24,25] as adsorbent/refrigerant working pairs.

In the case of Metal Hydride Cooling Systems, different cycles have been conceived [24] and, actually, a number of configurations have been proposed in the literature as evolutions of the basic and simplest "single stage - single effect" cycle reported in Fig. 11. On the basis of a thermal cycle properly designed for the application [26], the developed metal hydride-composite materials have been consolidated as fixed beds inside aluminium alloy cylindrical reactors, properly designed to optimize heat exchanging during hydriding/de-hydriding reactions of the active material. Finally, the heat exchangers have been engineered to develop a Metal Hydride based Cooling System (MHCS). Using the waste heat produced by the thermal engine as energy source, the MHCS has been implemented as cold generator into a prototype vehicle prepared for refrigerated transportation. Two views of the developed prototype can be seen in Fig. 12. In the vehicle, the thermally insulated van (see Fig. 12, bottom view) is refrigerated by the chilled water coming from the cold bed. At the present the vehicle is under testing and performance data are in course of acquisition. A more detailed description of technical aspects of the vehicle implementation is outside the aim of this work, and can be found in Ref. [27]. With reference to the cooling phase of the cycle regarding the production of cooling power, in this paper only some preliminary data obtained from the functional tests of the refrigerated prototype are reported.

Fig. 13 shows temperature values measured on the cold bed during the active refrigerating step. The a and b curves represent the inlet and the outlet temperatures of the heat exchanging water and the c and d curves represent the temperature of the cold bed, at the two ends of the tube, respectively. At the beginning of the phase the water and the cold bed temperatures are close to ambient (about 30 °C). At the opening of the hydrogen valves a flow of hydrogen from the cold bed to the hot bed is promoted and the hydrided material inside the cold bed desorbs hydrogen. The endothermic characteristic of the dehydriding process promotes the cooling of the bed, as evidenced by the decreased temperature values in the figure. Water temperatures decreasing also observed in the graph is due the circulation of the water coming from the heat exchanger.

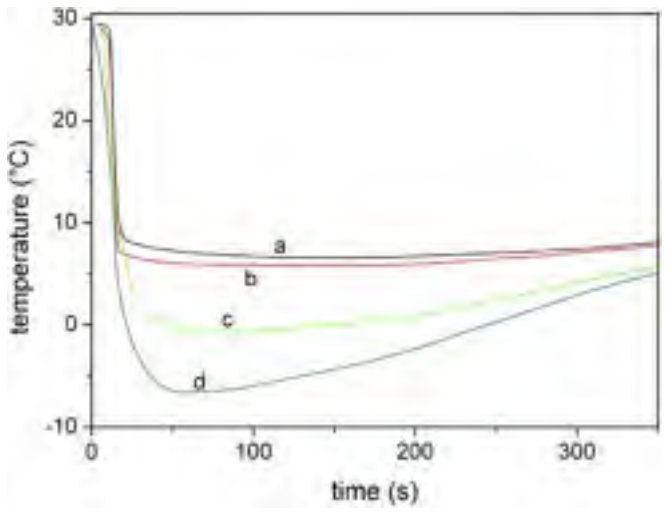

Fig. 13. Thermal behaviour of cold bed in the active refrigerating phase of the Metal Hydride Cooling System. The curves a and b represent the inlet and the outlet temperatures of the heat exchanging water in function of the time. The curves c and d represent the temperature values in function of the time as measured inside the cold bed at the two ends of the cyclindrical reactor containg the active material.

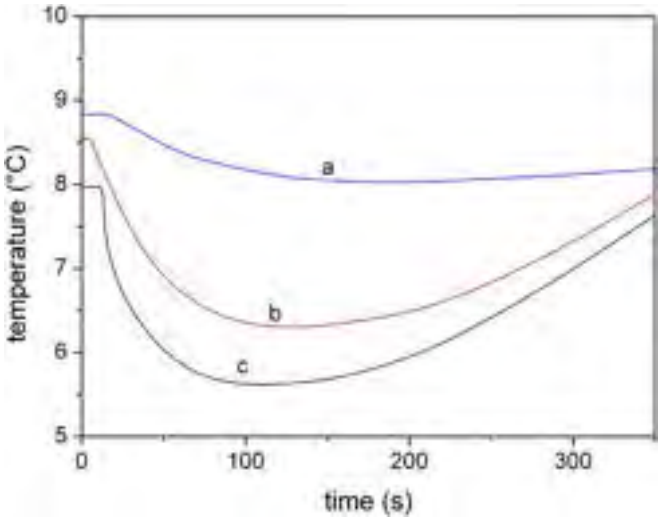

Fig. 14. Cooling effect of the Metal Hydride Cooling System during the active refrigerating phase. The curve a represents the temperature values measured inside the refrigerated van in function of the time. The curves b and c represent the temperature values as mesured for the inlet and outlet cooling water circulating into the internal heat exchanger placed inside the refrigerated.

Fig. 14 shows the temperature values registered in the refrigerated van (curve a) and in the cooling water in (curve b) and out (curve c) the heat exchanger placed inside the refrigerated van as a function of the time. From the figure, we can observe that the phase is closed when the heat exchanges become almost insignificant. The implemented cycle reaches a minimum temperature value less than 10 °C in the refrigerated compartment, being the duration of the useful phase of about 360 s. Although the minimum obtained temperature value does not appear to fully fit the requirements for refrigerated transportation, the developed device is clearly able to cooling down the temperature of the closed van demonstrating that the MHCS can be reasonably exploited in less critical applications.

4. Conclusion

An innovative methodology based on the combination of ball milling and extrusion techniques is reported. The process permits to obtain a metal hydride-based composite material at high metal hydride content (85% weight) with enhanced thermal conductivity and mechanical stability. The exhibited λ value around 2.0 W/mK ensures the required heat transfer also during the phases of a thermal cycle operating at low pressure. This constitutes a favourable condition to use the composite in developing sorption-based technologies. The composite is currently under further testing to quantitatively assess the behaviour after repeated hydrogen cycling. In addition, with respect to traditional fixed bed of particles, the composite in form of pellets can be easily handled and fixed in beds with various geometries. Several AB5 alloys were processed by the new approach and characterization results are reported. Results obtained for the AB5 alloys can be extended to other metal alloys and the material processing approach can be quite easily scaled up due to the intrinsic features of the applied

Please cite this article in press as: M. Pentimalli, et al., Nanostructured metal hydride – Polymer composite as fixed bed for sorption technologies. Advantages of an innovative combined approach by high-energy ball milling and extrusion techniques, Renewable Energy (2016), http://dx.doi.org/10.1016/j.renene.2016.07.074

high-energy ball milling and extrusion techniques. Composite materials at different compositions have been utilised as hydriding fixed bed and engineered into a metal hydride based cooling system able to produce cooling energy. Finally, the system was applied to the development of a refrigerated transportation vehicle and the prototype is currently under testing.

Preliminary results assess the operability of the prototype and constitute the starting point for the successive optimization of the system, also for different applications.

Acknowledgments

Part of this work was carried on in the frame of the FP7-SME-2012 Research for SMEs, HP-ACS project, grant no. 315103.

References

[1] Y. Nakamura, K. Sato, S. Fujitani, K. Nishio, K. Ogur, I. Uehara, Lattice expanding behaviour and degradation of $LaNi_5$-based alloys, J. Alloy Compds. 267 (1998) 205–210.
[2] J.-M. Joubert, M. Latroche, R. Cerny, A. Percheron-Guégan, K. Yvon, Hydrogen cycling induced degradation in $LaNi_5$-type materials, J. Alloy Compd. 330–332 (2002) 208–214.
[3] H. Ishikawa, K. Oguro, A. Kato, H. Suzuki, E. Ishii, Preparation and properties of hydrogen storage alloy-copper microcapsules, J. Less Common Metals 107 (1985) 105–110.
[4] F. Watanabe, C. Ikai, M. Hasatanti, C. Marumo, Hydration characteristics of metal hydride fixed in resin form, J. Chem. Eng. Jpn. 25 (1992) 1–5.
[5] Y. Uemura, R. Yasutsune, Y. Hatate, Encapsulation of hydrogen storage alloy by polymer, J. Chem. Eng. Jpn. 24 (1991) 377–381.
[6] S.S. Moon, K.S. Nahm, An improvement in the properties of hydrogen storage alloy by copper microencapsulation, J. Alloy Compd. 224 (1995) 140–147.
[7] T. Akiyama, T. Tazaki, R. Takahashi, J. Yagi, Optimization of microencapsulating and compacting conditions for hydrogen storage alloy, J. Alloy Compd. 236 (1996) 171–176.
[8] L.K. Heung, G.G. Wicks, G.L. Enz, Composition for Adsorbing Hydrogen, U.S. Patent 5,411,928/A, 2 May 1995.
[9] L.K. Heung, G.G. Wicks, Silica embedded metal hydrides, J. Alloy Compd. 293–295 (1999) 446–451.
[10] M. Pentimalli, F. Padella, A. La Barbera, L. Pilloni, E. Imperi, A metal hydride-polymer composite for hydrogen storage applications, Energy Convers. Manag. 50 (2009) 3140–3146.
[11] M. Pentimalli, F. Padella, L. Pilloni, E. Imperi, P. Matricardi, AB5/ABS composite material for hydrogen storage, Int. J. Hydrogen Energy 34 (2009) 4592–4596.
[12] M. Pentimalli, A. Frazzica, A. Freni, E. Imperi, F. Padella, Metal hydride-based composite material with improved thermal conductivity and dimensional stability properties, Adv. Sci. Technol. 72 (2010) 170–175.
[13] M. Pentimalli, E. Imperi, M. Bellusci, C. Alvani, A. Santini, F. Padella, Silica-metal composite for hydrogen storage application, Crystals 2 (2012) 690–703, http://dx.doi.org/10.3390/cryst2020690.
[14] D.E. Dedrick, Solid-state hydrogen storage system design, in: Gavin Walker (Ed.), "Solid State Hydrogen Storage: Materials and Chemistry", Woodhead Publishing LTd, Cambridge, 2008.
[15] R. de Boer, S.F. Smeding, Thermally operated mobile air-conditioning system, Development and test of a laboratory prototype, Paper presented at the International Sorption Heat Pump Conference, Seoul, Korea, 20.
[16] R. de Boer, S.F. Smeding, S. Mola, Silica gel-water adsorption cooling prototype system for mobile air conditioning, Paper presented at the Heat Powered Cycles Conference, Berlin, 200.
[17] M. Verde, J.M. Corberan, R. de Boer, S.F. Smeding, Modelling of a waste heat driven silica gel/water adsorption cooling system comparison with experimental results, Paper presented at the International Sorption Heat Pump Conference, Padua, Italy, 2011.
[18] L.Z. Zhang, Design and testing of an automobile waste heat adsorption cooling system, Appl. Therm. Eng. 20 (1) (2000) 103–114.
[19] Y. Zhong, Size reduction of an engine waste-heat driven air- conditioner for passenger cars and light-duty trucks, Energy Procedia. 14 (0) (2012) 351–357.
[20] W.-D. Wu, H. Zhang, C.-l Men, Performance of a modified zeolite 13X-water adsorptive cooling module powered by exhaust waste heat, Int. J. Therm. Sci. 50 (10) (2011) 2042–2049.
[21] S. Jiangzhou, R.Z. Wang, Y.Z. Lu, Y.X. Xu, J.Y. Wu, Experimental study on locomotive driver cabin adsorption air conditioning prototype machine, Energy Convers. Manag. 46 (9–10) (2005) 1655–1665.
[22] R.E. Critoph, S.J. Metcalf, Z. Tamainot-Telto, Proof of concept car adsorption air conditioning system using a compact sorption reactor, Heat. Transf. Eng. 31 (11) (2010) 950–956.
[23] Z. Tamainot-Telto, S.J. Metcalf, R.E. Critoph, Novel compact sorption generators for car air conditioning, Int. J. Refrig. 32 (4) (2009) 727–733.
[24] P. Muthukumar, M. Groll, Metal hydride based heating and cooling systems: a review, Int. J. Hydrogen Energy. 35 (8) (2010) 3817–3831.
[25] F.S. Yang, G.X. Wang, Z.X. Zhang, X.Y. Meng, V. Rudolph, Design of the metal hydride reactors-a review on the key technical issues, Int. J. Hydrogen Energy 35 (8) (2010) 3832–3840.
[26] HP-ACS project "Metal Hydride Heat Pump for Waste Heat Recovery in Vans Refrigeration Systems". FP7-SME-2012, grant n. 31510.
[27] http://cordis.europa.eu/project/rcn/108147_en.html.

Please cite this article in press as: M. Pentimalli, et al., Nanostructured metal hydride – Polymer composite as fixed bed for sorption technologies. Advantages of an innovative combined approach by high-energy ball milling and extrusion techniques, Renewable Energy (2016), http://dx.doi.org/10.1016/j.renene.2016.07.074

SOLVING COMPRESSED AIR SYSTEMS' ENERGY PUZZLE: HOW DOES YOUR SYSTEM STACK UP?

EPSRC Centre for INDUSTRIAL SUSTAINABILITY

Problem statement

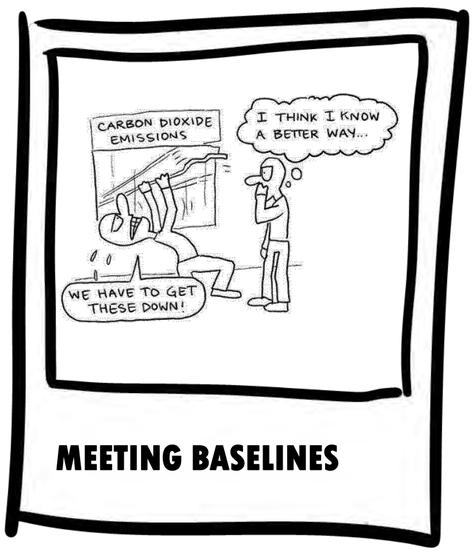

Compressed Air Systems (CAS) cover from 10% up to 70% of total industrial plants' electricity consumption. Only the 10% of the energy consumed to produce compressed air gets to the point of use.

But how are we dealing with CAS' energy efficiency? Are we producing, distributing and using compressed air in the most efficient way in relation to our process' needs? Tools to easily and effectively assess and benchmark system's performance and ongoing progress are still lacking.

Methodology

Preliminary results and discussion

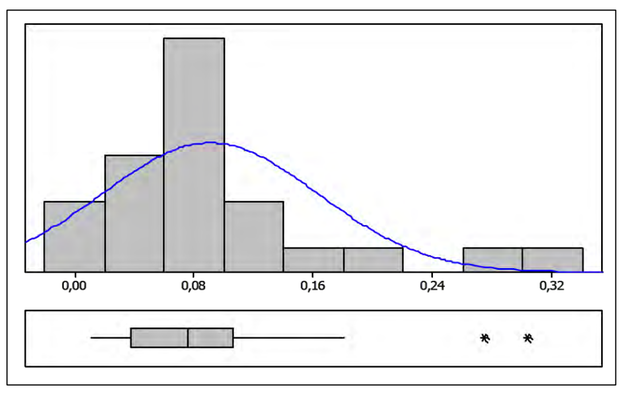

Ratio between the CAS's and the total electricity consumption (sectorial, manufacture of basic metals shown as an example).

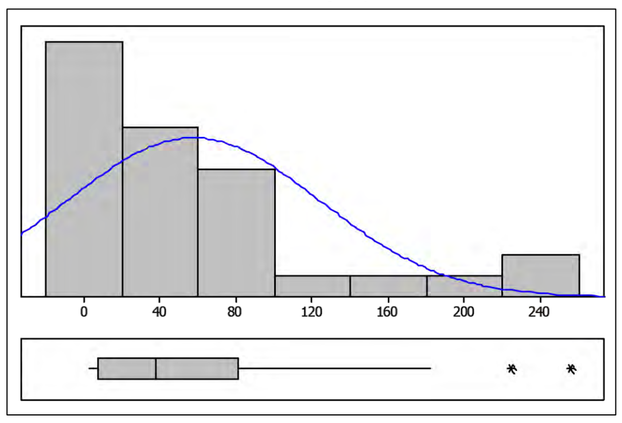

Ratio between the CAS's electricity consumption and the production volumes in tons (sectorial, manufacture of basic metals shown as an example).

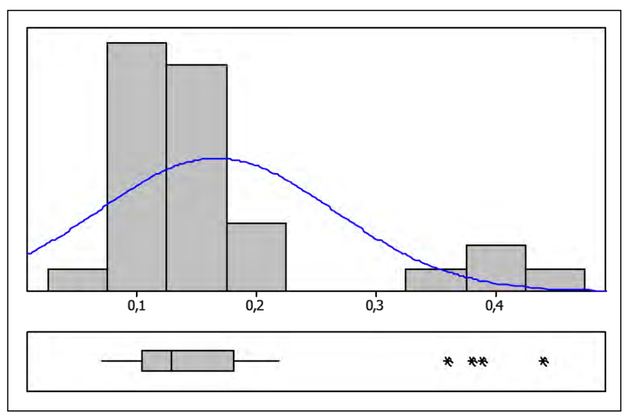

Ratio between the CAS's electricity consumption and the produced compressed air (cross-sectorial).

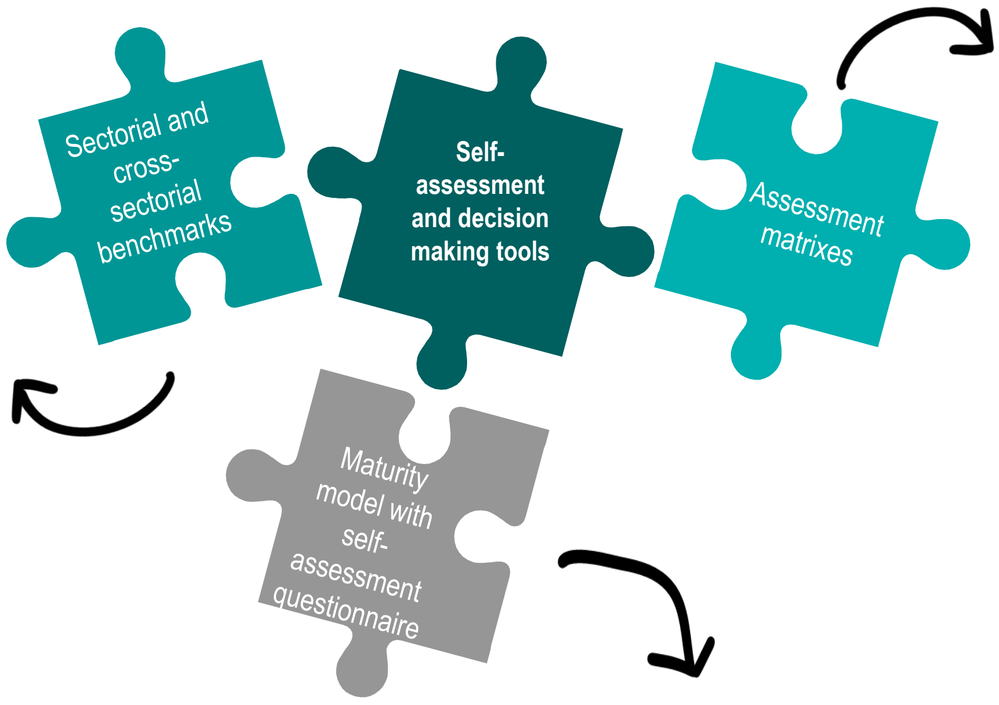

The maturity model is structured into 5 levels and 4 dimensions. Results of the self-assessment questionnaire are given as % coverage of dimensions and levels. Improvement actions are suggested considering that dimensions' development should be as symmetrical as possible and % coverage of levels should be higher for lower levels, and help you defining a development path.

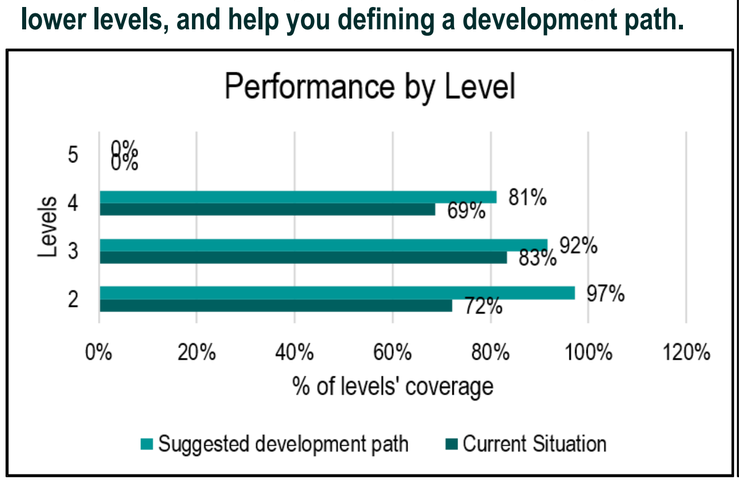

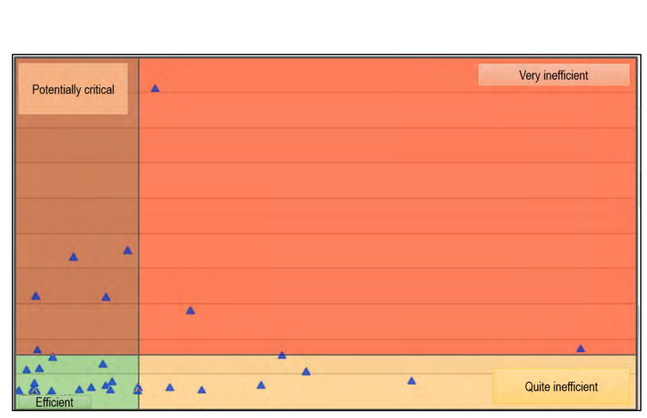

Assessment matrixes allow you to compare your plant's performance to other plants' (blue triangles) within the same sector or subsector. They are scatterplots of CAS's actual consumption vs the efficiency ratio, i.e. the ratio between CAS's actual consumption and CAS's consumption as predicted by the regression with production volumes. They take therefore into account differences due to different plant sizes.

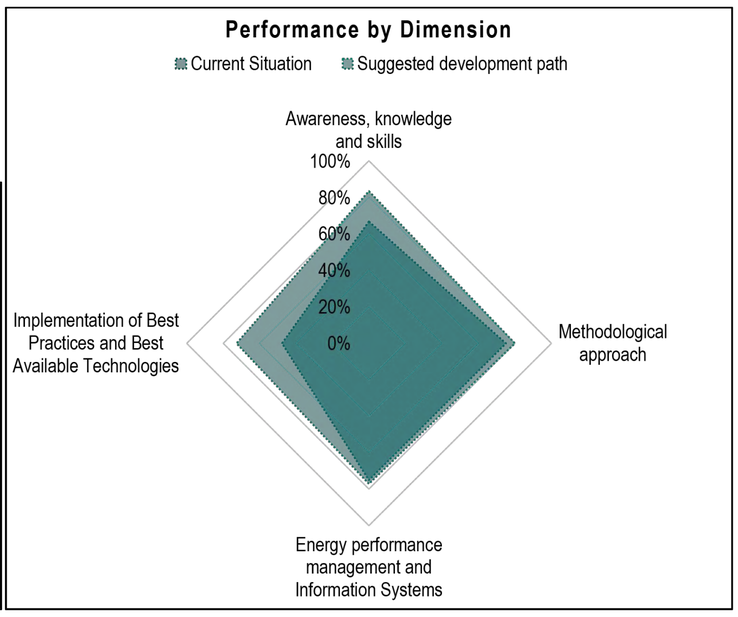

Key references

- Radgen P, Blaustein E. Compressed Air Systems in the European Union: Energy, Emissions, Savings Potential and Policy Actions. 2001.
- Phelan P, Chau D, Sarac H., Kaya D. Energy conservation in compressed-air systems. *Int J Energ Res* 2002;26:837–849.
- Saidur R, Rahim N, Hasanuzzaman M. A review on compressed-air energy use and energy savings. *Renew Sust Energ Rev* 2010;14:1135-1153.
- Dindorf R. Estimating Potential Energy Savings in Compressed Air Systems. *Procedia Engineering* 2012;39:204-211.
- Anglani N, Mura P. Optimization opportunities in compressed air production, distribution and use of compressed air in most relevant sectors (Opportunità di ottimizzazione dei consumi nella produzione, distribuzione, utilizzo dell'aria compressa nei settori industriali più sensibili). ENEA, 2010.
- U.S. DoE. Compressed Air Challenge. Improving compressed air system performance, a sourcebook for industry. 2003.

Miriam Benedetti | mb2132@cam.ac.uk | miriam.benedetti@uniroma2.it |

Supervised by:
Dr. Vito Introna (University of Rome "Tor Vergata", Department of Enterprise engineering)
Dr. Francesca Bonfà (ENEA, Italian Energy, New Technology and Environment Agency)

Available online at www.sciencedirect.com

SciVerse ScienceDirect

Energy Procedia 00 (2016) 000–000

Energy Procedia

www.elsevier.com/locate/procedia

The 8th International Conference on Applied Energy – ICAE2016

Assessing and improving Compressed Air Systems' energy efficiency in production and use: findings from an explorative study in large and energy-intensive industrial firms

Miriam Benedetti[a*], Ilaria Bertini[b], Francesca Bonfà[b], Silvia Ferrari[b], Vito Introna[c], Domenico Santino[b], Stefano Ubertini[d]

[a]*Department of Industrial Engineering, "Tor Vergata" University of Rome, Via del Politecnico, 1, 00133, Rome, Italy*
[b]*Energy, New Technology and Environment Agency (ENEA), Via Anguillarese 301, 00123 Rome, Italy*
[c]*Department of Enterprise Engineering, "Tor Vergata" University of Rome, Via del Politecnico, 1, 00133, Rome, Italy*
[d]*DEIM - School of Engineering, University of Tuscia, Largo dell'Universitá s.n.c., 01100 Viterbo,*
[*]*Corresponding author email: miriam.benedetti@uniroma2.it*

Abstract

Compressed Air Systems (CAS) are one of the most common and energy intensive utilities in industry, representing up to 10% of the industrial energy needs. Nevertheless, benchmarks currently available are usually based on nominal data and referred to the quality of the design, while there are still no available benchmarks based on measured industrial data, taking into consideration actual operating conditions, and referred to compressed air production and, most of all, use. In accordance with the Italian transposition of the European Directive 2012/27/EU (i.e. Legislative Decree 102/2014) large and energy-intensive enterprises have been asked to perform mandatory energy audits in 2015. In this context, a data collection focused on CAS has been carried out by means of a semi-structured questionnaire in the form of a spreadsheet. First data analyses performed and relative findings are here illustrated, together with the next steps for the creation of reliable sectorial and cross-sectorial benchmarks.

Selection and/or peer-review under responsibility of ICAE

Keywords: Energy Efficiency, Compressed Air Systems, Directive 2012/27/EU, energy benchmarking.

1. Introduction

With the promulgation of the Directive 2012/27/EU, a common framework of measures for the promotion of energy efficiency has been established in order to ensure the achievement of the European Union's energy efficiency improvement target of a 20% reduction of current primary energy consumption by 2020, and to pave the way for further energy efficiency improvements beyond that date. In this context, CAS play a strategic role in order to achieve the always more compelling objective of reducing the

industrial energy consumption in Europe as well as in the rest of the world [1, 2], due to their large diffusion in industrial plants [3] and to their energy intensity [3-6].

Italy has transposed the cited European Directive into national law by issuing the Legislative (Lgs.) Decree n°102 of the 4th July 2014. According to Art. 8 of such Decree, the large [8] and energy intensive (i.e. enlisted in the ad hoc list for the electricity sector of Cassa Conguaglio) enterprises must undergo energy audits on their plants at least every four years, starting from the first deadline that was 5 December 2015.

The implementation of the Lgs. Decree 102/2014 in 2015 has therefore been the perfect opportunity to gather CAS-related data in order to assess the current energy efficiency level of compressed air production and use in Italian industry, to define effective benchmarks and to enhance knowledge and best practices transfer among undertakings, thus contributing to the increment of CAS's energy efficiency. Data gathered were not limited to CAS, but first analyses were conducted on these systems due to their relevance from an energy efficiency point of view, as previously highlighted. As a matter of facts, only a few relevant and reliable benchmarks are available in the scientific and technical literature, as for example [4, 5, 8-10], but they are usually referred only to the production phase and are generally calculated in nominal conditions, not considering system's deterioration over time, specific operating conditions and also the influence of set points and demand fluctuations. This makes such information very unhandy and often confusing for companies. In such a context, a series of studies has been set up aimed at helping companies in the complex assessing, benchmarking and improving CAS's energy efficiency, and at providing them with accessible, easy and effective tools. Italian data have thus been used as a first data set to design such tools, and obtained results can be applied to the international context and extended where possible. The study presented in this paper is then the first step of a broader research framework, and the process for collecting data regarding CAS's energy efficiency is described, along with the data analysis methodology used and first findings

2. Methodology

Data analyses have been initially limited to the following nine industrial sectors, selected for their intensive use of compressed air, on the basis of existing literature [9, 10]: manufacture of basic metals, chemicals and chemical products, basic pharmaceutical products and pharmaceutical preparations, fabricated metal products except machinery and equipment, motor vehicles, plastics products, textiles, food products, paper and paper products [11].

Target organizations have been asked to complete a voluntary semi-structured questionnaire in the form of a spreadsheet, and to submit it together with the mandatory documentation. The questions asked in the spreadsheet are summarized in Table 1. The collected variables are production volumes, total electrical consumption, indicated as kWhe TOT, amount of energy consumed for the production of compressed air, indicated as kWhe CAS, and value of the main energy driver. Such variables are all referred to the year 2014. Given the exploratory nature of this first study, no power analysis and sample size calculation was performed in a preliminary fashion.

Data analyses have been mainly performed on derived variables calculated as follows:

- The ratio between the amount of energy consumed for the production of compressed air and the total electrical consumption (kWhe CAS/kWhe TOT);
- The ratio between the amount of energy consumed for the production of compressed air and the production volumes, generally expressed as tons of final product (kWhe CAS/t);

The ratio between the amount of energy consumed for the production of compressed air and the value of the main energy driver, generally expressed as m^3 of compressed air produced (kWhe CAS/m^3).

First of all, the distribution of the collected variables has been analyzed and its normality has been tested with the Anderson-Darling test [12]. Then, variables have been examined by calculating descriptive

statistics (frequencies, percentages, averages, medians, standard deviation and confidence of intervals at 95%). To compare industries' sub-sectors, the Welch's One-Way ANOVA test [13] has been used to evaluate differences in the means of continuous variables. This test has been selected for its wide applicability, as it does not assume data sets to be normally distributed if they have an adequate size or to have similar standard deviations. Statistical tests have been performed accepting a probability value (P-value) ≤ 0.05. Such analyses have been performed for each industry and also repeated for industries' subgroups limited to those that have provided continuously measured data, except for the Welch's One-Way ANOVA test due to the restricted samples size. Analyses regarding the kWhe CAS/m^3 derived variable have only been conducted on subgroups, as non-measured data seemed useless in this case, and cross-sectorial, in order to avoid problems due to restricted sample size.

3. Data analysis results

In this section, the results of the data analysis are presented in details for the manufacture of basic metals in order to give a complete description of the presented methodology's application, while they are only briefly summarized for the other analysed sectors.

For the manufacture of basic metals, 223 questionnaires have been analysed. Of the corresponding 223 plants, 195 gave an estimation or a measure of the value of the amount of energy consumed for the production of compressed air. The highest percentage of questionnaires was returned by undertakings belonging to the casting of metal sub-sector (over 40%) and the rest of them belongs to other 4 sub-sectors or did not declare it (over 20%). Table 1 summarises the percent breakdown of responses to each question.

Table 1. Questions and percent breakdown of responses

Questions	Possible answers	Percent
Methodology adopted for estimating total electrical consumption	Calculated from energy bills	17%
	Spot measures	4%
	Continuous measures provided by dedicated meters	70%
	Undeclared	9%
Methodology adopted for estimating the energy consumed for the production of compressed air	Calculated from energy bills	69%
	Spot measures	3%
	Continuous measures provided by dedicated meters	14%
	Undeclared	14%
Please indicate the main energy driver you use to evaluate the performance of your compressed air system	Compressed air production	35%
	Others	1%
	Undeclared	64%
Methodology adopted for estimating values related to the main energy driver for your compressed air system	Calculated on the basis of nominal system's parameters or of physics	28%
	Spot measures	1%
	Continuous measures provided by dedicated meters	4%
	Undeclared	67%

In the plots shown in Figure 2, results for normality test and descriptive statistics of main variables and derived variables are represented for groups of data comprehending continuous measures only (see Figure 3 for a summary of the results obtained for the whole sample). Only plants measuring production volumes in weight have been considered in order to analyze the ratio between the amount of energy consumed for the production of compressed air and the production volumes due to the fact that they are above 90% of the total.

The results of Welch's One-Way ANOVA are not plotted for sake of brevity, but they show that there is no significant difference in the mean value of the analysed variables and derived variables of plants belonging to different sub-sectors.

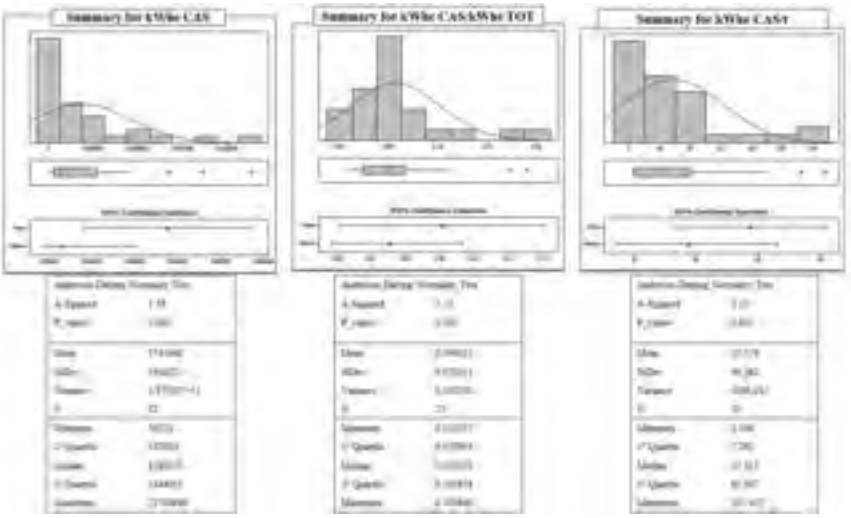

Fig. 2. Manufacturing of basic metals: normality test and descriptive statistics of main variables and derived variables for groups of data comprehending continuous measures only.

The main results of the data analysis are summarized in the matrix shown in Figure 4, reporting the various industries on columns and questions, variables and derived variables on rows. The green colour in the cells of the matrix means that values of answers, variables and derived variables highlight a satisfying amount of data collected or a relevant probability of profitably implement energy efficiency measures. Red colour means the opposite. Median values rather than means have been analysed, in order to obtain more reliable results, as several industries showed a relevant amount of outliers that have still got to be interpreted. The last row of the matrix shows the impact of the amount of energy consumed by CAS in each industry on the national industrial energy consumption (calculated according to data reported by [14]). In the following Figure results of the kWhe CAS/m^3 derived variable are reported.

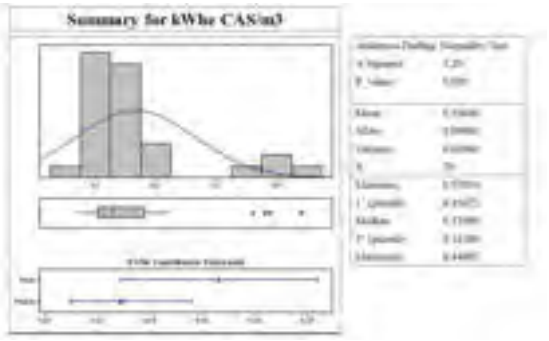

Fig. 3. Results of the analysis conducted on the ratio between the amount of energy consumed for the production of compressed air and the compressed air produced.

			Basic metals	Chemicals	Pharmaceutical	Fabricated metal products	Motor vehicles	Plastics products	Textiles	Food products	Paper
AMOUNT OF DATA COLLECTED		Number of analysed questionnaires	223	208	105	315	72	228	132	385	95
		Number of plants continuously measuring kWhe TOT	156	134	64	191	47	151	82	265	71
		Number of plants continuously measuring kWhe CAS	32	30	10	19	7	17	6	38	9
		Number of plants continuously measuring m3 of compressed air produced	9	16	6	6	7	5	3	11	2
PROBABILITY OF PROFITABLY IMPLEMENT ENERGY EFFICIENCY MEASURES	GROUPS OF DATA COMPREHENDING CONTINUOUS MEASURES	kWhe CAS	1281079	1629138	924103	504000	1558550	785342	521500	951221	38812468
		kWhe CAS/kWhe TOT	0,08	0,12	0,05	0,10	0,10	0,07	0,05	0,07	0,04
		kWhe CAS/m3	0,13	0,12	0,16	0,13	0,13	0,00	0,10	0,14	0,17
		kWhe CAS/t	37	16	831	35	255	143	51	21	23
	WHOLE SAMPLE	kWhe CAS	506920	517216	410253	272411	530982	341521	245410	285488	459228
		kWhe CAS/kWhe TOT	0,07	0,08	0,05	0,09	0,12	0,06	0,06	0,06	0,04
		kWhe CAS/t	44	24	1405	59	92	50	119	18	18
		Incidence of CAS energy consumption on national industrial energy consumption	1,23%	0,97%		1,23%	0,27%	0,32%	0,19%	0,58%	0,25%

Fig. 4. Summary of the main results of the data analysis for all analyzed industries.

4. Discussion

Results from the data analysis led to the drawing of a first set of findings. First of all, the dramatically low percentage of plants measuring the kWhe CAS as well as the amount of produced compressed air is an effective indicator of the still too little attention paid to energy management in Italian industrial plants. Despite the high energy cost related to compressed air production, energy measuring, controlling, budgeting and forecasting are still rarely performed, not even in highly energy intensive systems. Therefore, the development of energy measuring systems should be considered as a priority over the next few years. CAS appear to be a significant energy use in most industries, as the kWhe CAS/kWhe TOT derived variable ranges from 4% to 12%, with a mean value across different industries of about 7%. They also cover a significant percentage of the national industry consumption (i.e. a total of 5% considering all analyzed industries).

The kWhe CAS/t derived variable seems to be a promising indicator for CAS energy efficiency within a single industry, as it appears to have a non-scattered distribution, while it cannot definitely be used to compare different industries. This is probably due to different processes required by different products. Looking at Figures 2 and 3, it is possible to observe how plants showing anomalous behaviors are easily

identifiable and also represent a small percentage of the total. Once the energy efficiency situation of these plants will be analyzed, evaluating whether different performances are due to different systems' efficiency or to different operational parameters' settings, it will be possible to repeat the analysis on the same sample and verify the reliability of those values and distributions as benchmarks.

The kWhe CAS/m^3 is instead a good cross-sectorial indicator of the energy efficiency in the production of compressed air, but it does not allow measuring the energy efficiency in the consumption of such a vector. An indicator such as the amount of compressed air used to produce a single ton of product would be useful, but the restricted number of plants measuring compressed air still does not allow its calculation. Anyway, Figure 3 shows that the range of the kWhe CAS/m^3 value is slightly above the one proposed by [8], which is probably due to the fact that the latter does not consider real use operating conditions. There is also a small number of plants showing a much higher range, probably because they have different pressure requirements (to be confirmed through deeper analyses).

5. Conclusions and future developments

First findings from an explorative study aimed at assessing CAS's energy efficiency and defining reliable and robust benchmarks have been presented. On the average, less than 20% of analyzed plants measure kWhe CAS and about 7% of them measure m^3 of produced compressed air. CAS appear to be a significant energy use in most companies, covering on average the 7% of kWhe TOT. Most promising benchmarking indicators for both compressed air production and use and their calculation have been illustrated, along with their first application to a selected number of industries. By refining and completing the presented analysis (also using its results to identify more specific information to be gathered) and through the proposed methodology, it will be possible to define cross-sectorial and industry-specific CAS energy efficiency benchmarks, enabling and enhancing a more efficient knowledge and best practices transfer among undertakings.

Acknowledgements

This work is part of the Electrical System Research, implemented under Programme Agreements between the Italian Ministry for Economic Development and ENEA, CNR, and RSE S.p.A. The authors would like to thank all the companies that have kindly provided data and supported the project. Warm thanks also to Green Energy Plus S.r.l. that has provided useful feedbacks during the whole project.

References

[1] Introna V, Cesarotti V, Benedetti M, Biagiotti S, Rotunno R. Energy Management Maturity Model: an organizational tool to foster the continuous reduction of energy consumption in companies. *J Cle Prod* 2014;83:108-117.

[2] Benedetti M, Cesarotti V, Introna V, Serranti S. Energy consumption control automation using Artificial Neural Networks and adaptive algorithms: Proposal of a new methodology and case study. *Appl Energ* 2016;165:60-71.

[3] Radgen P, Blaustein E. Compressed Air Systems in the European Union: Energy, Emissions, Savings Potential and Policy Actions. 2001.

[4] Phelan P, Chau D, Sarac H., Kaya D. Energy conservation in compressed-air systems. *Int J Energ Res* 2002;26:837–849.

[5] Saidur R, Rahim N, Hasanuzzaman M. A review on compressed-air energy use and energy savings. *Renew Sust Energ Rev* 2010;14:1135-1153.

[6] Dindorf R. Estimating Potential Energy Savings in Compressed Air Systems. *Procedia Engineering* 2012;39:204-211.

[7] European Commission. *The new SME definition, User guide and model declaration*. 2005.

[8] European Commission. *Reference document on Best Available Techniques for Energy Efficiency*. 2009.

[9] Anglani N, Mura P. *Optimization opportunities in compressed air production, distribution and use of compressed air in most relevant sectors* (Opportunità di ottimizzazione dei consumi nella produzione, distribuzione, utilizzo dell'aria compressa nei settori industriali più sensibili). ENEA, 2010.

[10] U.S. DoE. *Compressed Air Challenge. Improving compressed air system performance, a sourcebook for industry*. 2003.

[11] EUROSTAT. *NACE Rev.2, Statistical Classification of economic activities in the European Community*. 2008

[12] Anderson T W, Darling DA. Asymptotic theory of certain "goodness-of-fit" criteria based on stochastic processes. *Ann Math Stat* 1952;23:193–212.

[13] Welch BL. The generalization of "Student's" problem when several different population variances are involved. *Biometrika* 1947;34(1–2):28–35.

[14] TERNA. Electrical consumption in Italy, available at http://www.terna.it/ [accessed 29 May 2016].

IN792 DS superalloy: optimization of EB welding and post-welding heat treatments

Giuseppe Barbieri[1,a]*, Peiman Soltani[2,3,b], Saulius Kaciulis[2,c], Roberto Montanari[3,d] and Alessandra Varone[3,e]

[1] ENEA, Department for Sustainability of Production and Territorial Systems - Research Centre of Casaccia, 00196, Rome, Italy

[2] ISMN – CNR, P.O. Box 10, 00015 Monterotondo Stazione, Rome, Italy

[3] Department of Industrial Engineering, University of Rome-Tor Vergata, 00133 Rome, Italy

[a] giuseppe.barbieri@enea.it, [b] peiman.soltani@ismn.cnr.it, [c] saulius.kaciulis@ismn.cnr.it,

[d] roberto.montanari@uniroma2.it, [e] alessandra.varone@uniroma2.it

Keywords: superalloys, welding, electron beam, microstructure, post-welding treatments

Abstract. Electron beam (EB) welding has been used to realize the seams on 2 mm thick plates of directionally solidified (DS) IN792 superalloy. A grid of the samples has been prepared by varying the pass speed v from 1 to 2.5 m/min, while the other process parameters (power P = 1 kW, acceleration voltage T = 50 kV, beam current I = 20 mA) were kept constant. Experiments were carried out both at room temperature and with pre-heating at 200 °C or 300 °C.
Once found the best process conditions (pre-heating at 300 °C; v = 2.5 m/min) the effect of post-welding heat treatments at 700 and 750 °C for increasing time up to 2 hours has been investigated.

Introduction

Ni-based superalloys are widely used in the components (disks and blades) of aeronautic engines and gas turbines operating at the highest temperatures [1-2]. Their microstructure mainly consists of particles of the $L1_2$ ordered $Ni_3(Al,Ti)$ ’-phase embedded in the disordered -phase matrix [3]. During the service life, the mechanical parts made of superalloys operate under high stress and temperature in a quite aggressive environment, therefore, sometimes surface cracks form leading to sudden rupture. Since these mechanical components are extremely expensive, their repairing by welding is more advantageous than replacement, however it is not an easy task. In fact, the welds must satisfy strict requirements: (i) modifying as little as possible the original microstructure; (ii) do not introduce in the molten (MZ) and heat affected (HAZ) zones any relevant residual stress; (iii) do not produce cracks in the MZ and HAZ; (iv) do not cause a massive surface segregation; (v) to minimize the elemental diffusion which can change consequently the chemical composition of and ’ phases.

The present work is a part of general project aimed to determine the optimal conditions for joining Ni base superalloys by means of high energy density welding techniques [4-7]; here electron beam (EB) welding was used to produce the seams on 2 mm thick plates of IN792 directionally solidified (DS) alloy. In comparison with other welding techniques, EB permits to get the narrower seams with lower heat input and reduced extension of MZ and HAZ. Since welding operations are carried out in high vacuum, a further advantage is the low gas absorption by liquid metal.

After EB welding, the microstructural features in the MZ, HAZ and base alloy have been investigated by micro-hardness tests, imaging by optical microscopy (OM) and scanning electron microscopy (SEM), X-ray diffraction (XRD) and Auger electron spectroscopy (AES), which has

already demonstrated its effectiveness in studies of composition profiles connected to diffusion phenomena in superalloys [8-9].

The last task of this work was to find a suitable post-welding heat treatment (PWHT).

Experimental

The nominal chemical composition of IN792 DS is: C 0.08, Cr 12.60, Co 9.0, Ta 4.0, W 4.0, Ti 4.0, Al 3.3, Mo 2.0, Hf 1.0, B 0.01, Ni to balance (wt %). The material has been supplied in form of cylindrical ingots (= 25 mm, L = 60 mm) with the [100] direction of the oriented grains parallel to the ingot axis. Plates of 2 mm thickness were obtained by spark-erosion cutting along the ingot axis.

EB welding has been performed both at room temperature and with pre-heating of the plates at 200 and 300 °C. Pre-heating was made by defocusing and wobbling the electron beam.

A grid of the samples has been prepared by varying the pass speed from 1 to 2.5 m/min keeping constant the other process parameters: power = 1 kW, acceleration voltage = 50 kV, beam current = 20 mA. First, the seams have been checked by X-ray radiography to identify possible macro-defects, such as porosities, cracks, etc., then they have been examined by OM and SEM to investigate the morphology, size and distribution of and ' phases and Vickers micro-hardness tests.

XRD measurements were carried out by focussing the beam on the base alloy, HAZ and MZ in order to determine the corresponding fraction of ' phase and the average size of ordered particles. The 110 superlattice and 220 fundamental reflections have been collected by using Mo-K radiation (= 0.7093 Å) with 2 angular intervals of 0.005° and counting times of 30 s per step.

Finally, the micro-chemical distribution of alloying elements in the different zones has been determined through AES multipoint analysis. AES measurements were carried out by a LEG200 electron gun mounted on the analysis chamber of an Escalab MkII and operated at 10 keV beam energy. Before the measurements, the surface was cleaned by using an Ar^+ ion gun at 2.0 keV energy in order to remove the first few monolayers of contaminants. AES experimental data were processed by the Avantage v.5 software.

Once identified the best EB process conditions, the samples were submitted to PWHT at 700 and 750 °C for increasing time up to 2 hours.

Results and Discussion

A first experimental run was carried out at room temperature, but EB joints always presented macro-defects like cracks and porosity (Fig.1 a). The cracks start from the seam centre, initially move along its axis, then divert of about 45°. SEM observations (Figs. 1 b-c) clearly show that the cracks follow the interdendritic boundaries, a typical feature of *hot tearing*. In Fig. 1 c), the particles of small size (~ 1 m) are also observed and EDS microanalysis revealed that they are Ti and Ta carbides. The combination of shrinkage stresses and micro-segregation arising from the solidification of the liquid between secondary dendritic arms (Fig. 1 d) leads to crack formation and its successive propagation along the easier way, i.e. the interdendritic boundaries. Of course, this phenomenon is favoured by high thermal gradients arising in EB welding, thus the successive tests have been made by pre-heating the material at 200 and 300 °C.

Figs. 2 (a-b-c) show the seams obtained with pre-heating temperature of 200 °C and pass speeds of 1.0 (a), 1.5 (b) and 2.0 m/min (c). Lower pass speeds involve higher thermal loads and consequently slower cooling rates during solidification which favour the formation of hot cracks. In the case of 1.0 m/min, Fig. 2 (a) shows a long crack along the seam axis that crosses the plate and emerges on the opposite side (see Fig.2 d). The cracks are not observed at higher pass speeds (b and c). Furthermore, the comparison between the cross-sections in e) and f) indicates that the aspect ratio *p/w* (*p* depth, *w* maximum width) increases with pass speed.

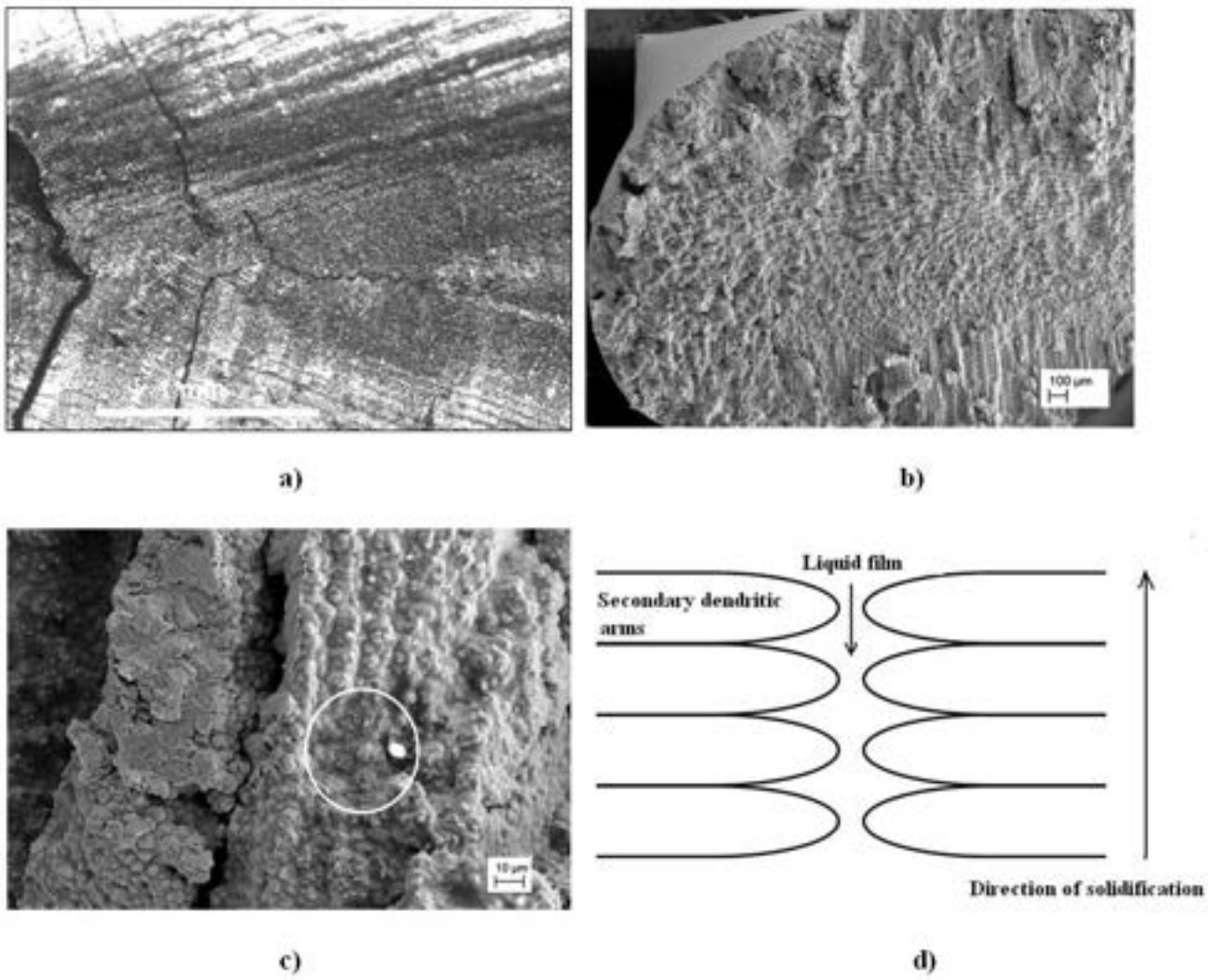

Fig. 1- Sample welded without pre-heating: cracks and pores are observed in the seam (a); fracture surfaces clearly show the dendritic structure (b-c). Schematic view of the mechanism leading to interdendritic fracture (d).

Figs. 3 (a-b-c) show the cross-sections of the seams obtained with pre-heating temperature of 300 °C and pass speeds of 1.5 (a), 2.0 (b) and 2.5 m/min (c). Also in this case, no cracks are observed and the aspect ratio improves as pass speed increases. From the morphological inspection, the optimal parameters for EB welding seem to be the following: pre-heating at 300 °C and pass speed of 2.5 m/min. The samples prepared in this way have been submitted to a thorough microstructural examination.

The amount of ’ phase in the MZ determined by XRD is ≈ 24 %, i.e. it is smaller than that of the base alloy, whereas this amount does not change in the HAZ. As expected, the ’ phase particles have a larger size in the HAZ than in the original alloy due to the strong heat flux around the seam that leads to the coarsening of the ordered phase. In the MZ, the ’ particles nucleate after solidification and have a very short growth time during the cooling to room temperature, thus their size is quite small and exhibit a round shape. Only few particles of about 60 nm can be observed by SEM whereas the larger part of them is quite finer: an average size of 20 nm has been calculated from the broadening of 110 superlattice XRD peak.

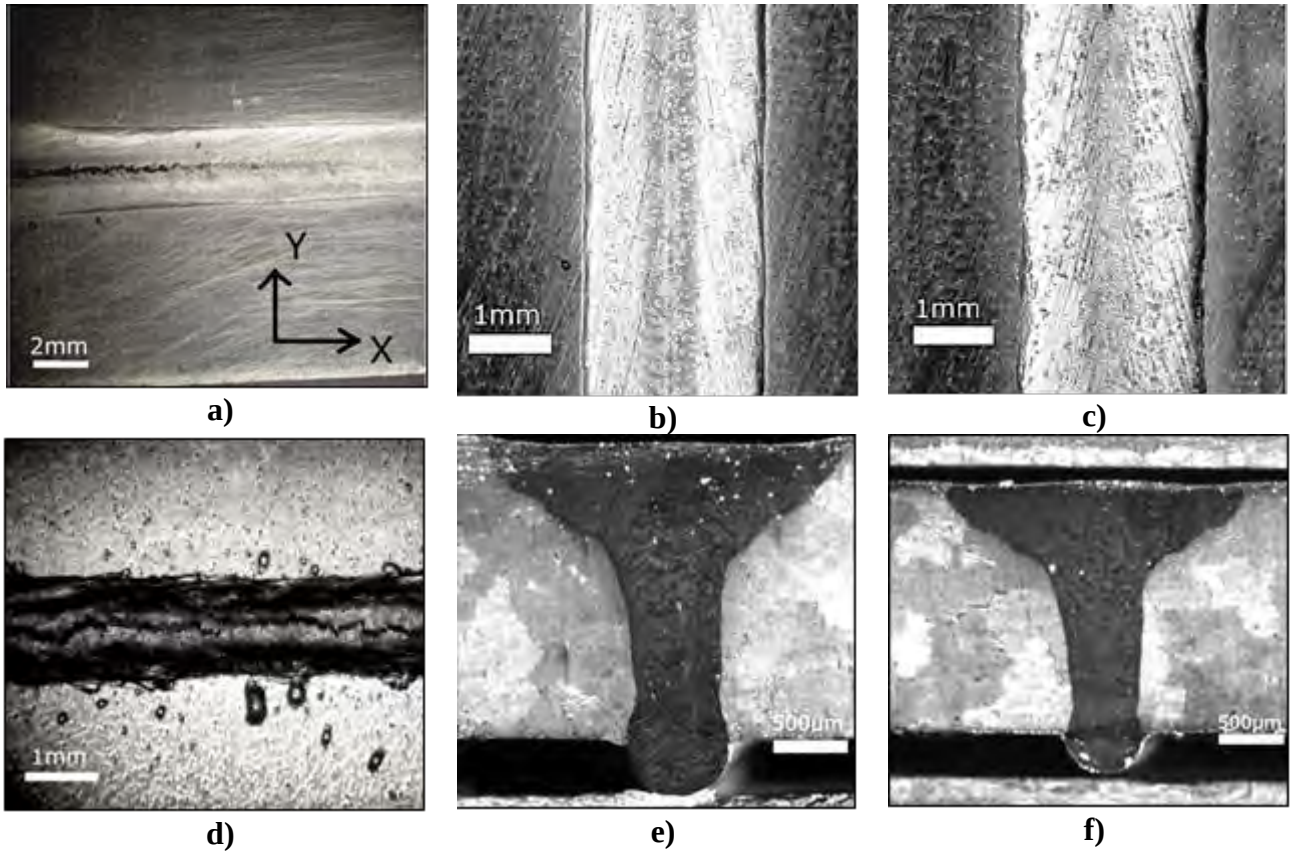

Fig. 2- Seams of the samples EB welded with pre-heating at 200 °C: pass speed of 1.0 m/min (a-d), 1.5 m/min (b-e) and 2.0 m/min (c-f). The image in d) is the opposite side of a). Cross-sections of the seams displayed in b) and c) are shown in e) and f), respectively.

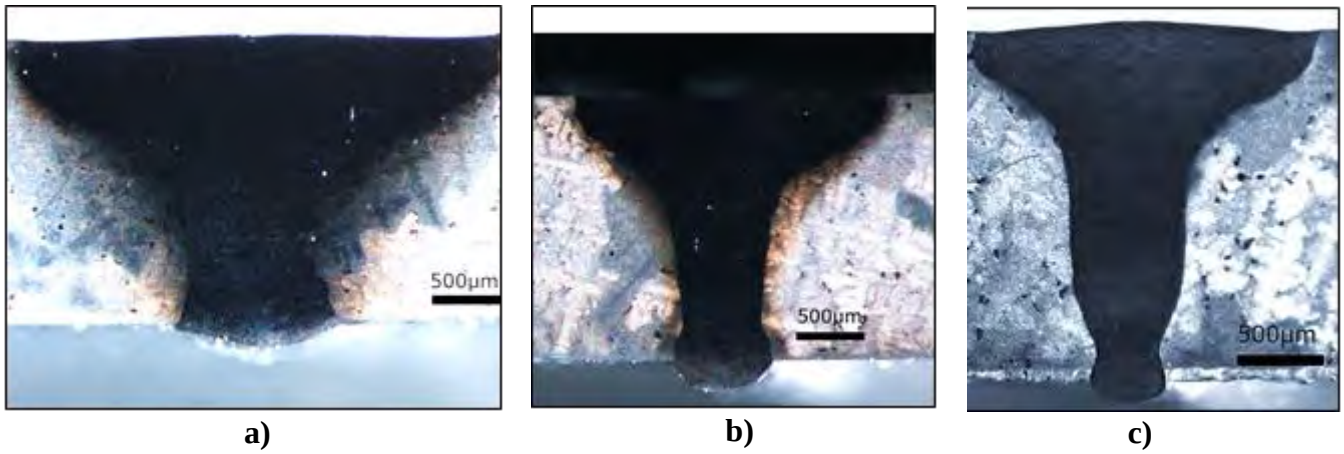

Fig. 3- Cross-sections of the seams obtained by EB welding with pre-heating at 300 °C: pass speed of 1.5 m/min (a), 2.0 m/min (b) and 2.5 m/min (c).

The excellent high temperature structural stability and properties of Ni base superalloys are mainly due to their complex composition. In particular, Cr, concentrated in phase, enhances the corrosion resistance while Mo, present is in both and ', plays an important role on lattice misfit; Ta and Hf are also added in IN 792 to control the ' volume fraction and the shape of carbides forming at grain boundaries, respectively. Therefore, the quality of welding strongly depends on the distribution of alloying elements. To evaluate the welding quality, the elemental line scans with much higher lateral resolution (about 0.5 m) have been performed by AES across the seam in

different positions on the surface. Typical trends of Ni, Cr, Ti and Mo concentrations in wt%, obtained by integrating the respective Auger peak areas, are reported in Fig. 4, where the start position of the scan corresponds to the centre of the seam.

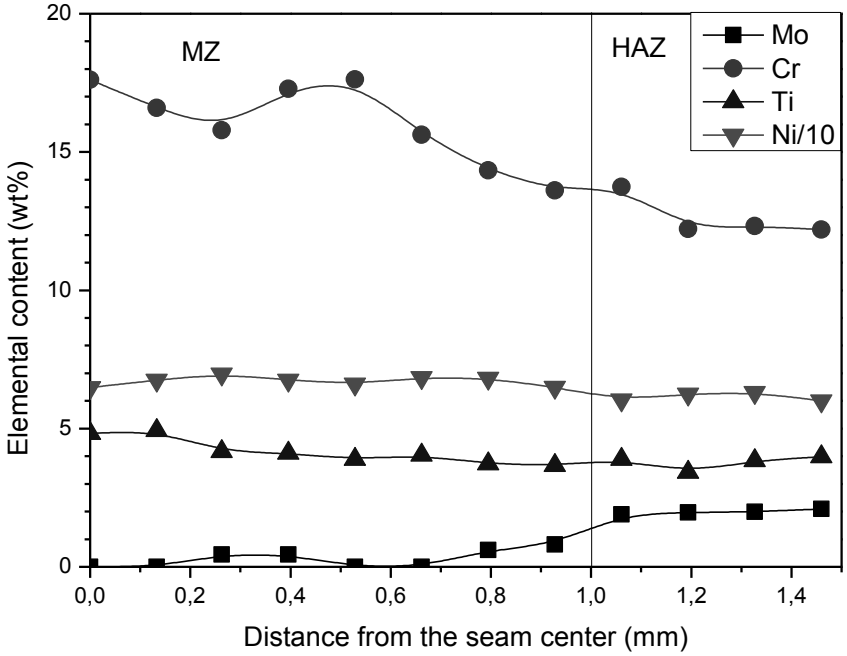

Fig. 4- EB welds obtained with pre-heating at 300 °C and pass speed of 2.5 m/min. Auger line scan of elemental content (wt%) determined from the Mo MNN, Cr LMM, Ti LMM and Ni LMM peak areas, respectively.

The amounts of Ni and Ti are almost constant through the scans, while some changes of Cr and Mo concentrations are observed in the MZ and HAZ. The amount of Mo equals to zero in the centre of the MZ and increases moving toward the HAZ, where it reaches a nearly stable value. The trend of Cr is opposite, i.e. it is decreasing from the centre of MZ. Such behaviour can be ascribed in part to the elemental diffusion in the liquid state and in part to the evaporation during EB passes. More details about micro-chemical analyses can be found in ref. [10].

The last task of this work was to find a suitable PWHT, therefore the samples welded with optimal EB process parameters have been treated at 700 and 750 °C for increasing time up to 2 hours.

Fig. 5 shows micro-hardness profiles across three parallel EB seams (1-2-3) measured after welding, heat treatments at 700 °C and 750 °C for 2 hours; the horizontal line indicates the mean value of the original material (430 HV).

In as-welded condition, the hardness of HAZ is always lower than the reference horizontal line and in some points the variation reaches 60 HV with a relative change of 14%. After both heat treatments, the profiles shift upwards with a remarkable improvement of hardness, however the peak-valley height is a little lower after 2 hours at 750 °C, i.e. the mechanical properties across the seam are more homogeneous.

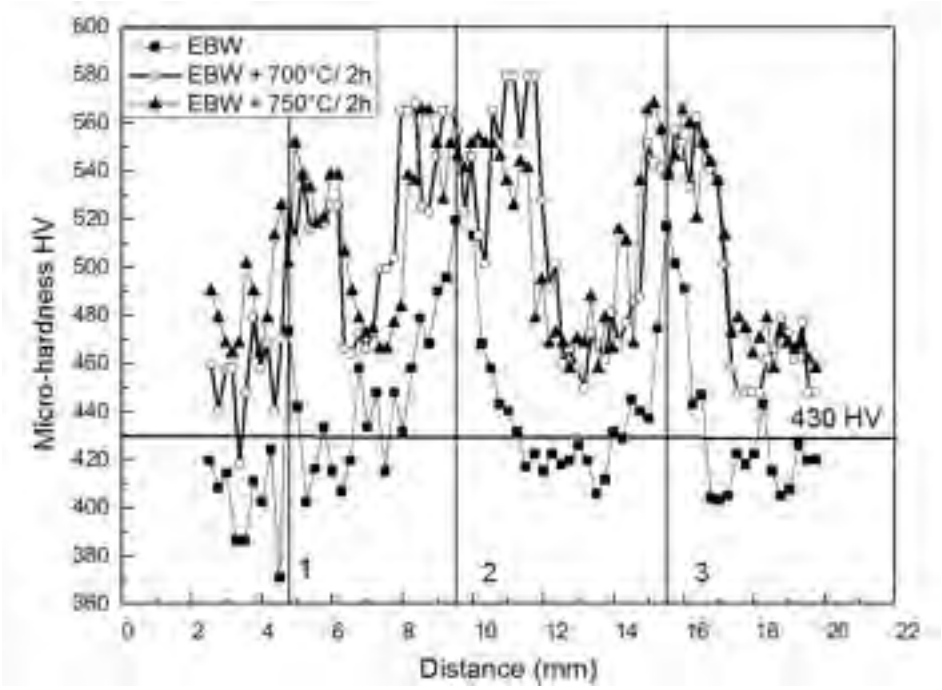

Fig. 5- Micro-hardness profiles across three parallel seams realized by EB welding with pre-heating at 300 °C. The different conditions are compared: as-welded, heat treated at 700 °C and 750 °C for 2 hours.

Conclusions

In order to identify the suitable process parameters, EB seams were realized on the plates of IN 792 DS superalloy in different conditions: (i) without and with pre-heating at 200 and 300 °C, (ii) by changing the pass speed from 1 to 2.5 m/min.

The results of present experiments indicated that the seams do not exhibit macro-defects (cracks and pores), if EB joints are realized with pre-heating and by using pass speeds not lower than 1.5 m/min. The microstructural examination of the samples showed that the best results are obtained with pre-heating at 300 °C and pass speed v = 2.5 m/min. The samples prepared with these process parameters were then heated at 700 and 750 °C for increasing time up to 2 hours.

Hardness of the original material is recovered after soaking time of 2 hours at both temperatures but the treatment at 750 °C guarantees better homogeneity.

References

[1] H. Monjati, M. Jahazi, R. Bahrami, S. Yue, Mater. Sci. Eng. A 373 (2004) 286-293.
[2] A.M. Ges, O. Fornaro, H.A. Palacio, Mater. Sci. Eng. A 458 (2007) 96-100.
[3] P. Deodati, R. Montanari, O. Tassa, N. Ucciardello, Mater. Sci. Eng. A 521-522 (2009) 102-105.
[4] M.T. Rush, P.A. Colegrove, Z. Zhang, B. Courtot, Adv. Mater. Res. 89-91 (2010) 467-472.
[5] Xiu-Bo Liu, Gang Yu, Jian Guob, Yi-Jie Gu, Ming Pang, Cai-Yun Zheng, Heng-Hai Wang, J. Alloy Comp. 453 (2008) 371-378.
[6] Huei-Sen Wang1, Chih-Ying Huang, Kuen-Sen Ho, Sian-Jhih Deng, Mater. Trans. 52-No. 12 (2011) 2197-2204.
[7] D.J. Tillack, Welding Journal 86 (2007) 28-32.
[8] S. Kaciulis, A. Mezzi, M. Amati, R. Montanari, G. Angella, M. Maldini, Surf. Interf. Anal. 44 (2012) 982-985.
[9] M. Amati, L. Gregoratti, S. Kaciulis, A. Mezzi, S.K. Balijepalli, R. Donnini, R. Montanari, G. Angella, G. Maldini, D. Ripamonti, La Metallurgia Italiana, 11-12 (2013) 1-6.
[10] R. Montanari, A. Varone, G. Barbieri, P. Soltani, A. Mezzi, S. Kaciulis, Surf. Interf. Anal. 2016 (in press).

Welding of Automotive Aluminum Alloys by Laser Wobbling Processing

Giuseppe.Barbieri[1, a *], Francesco Cognini[2,b], Massimo Moncada[2,c], Antonio Rinaldi[2,d], Gabriele Lapi[3,e]

[1]CALEF - Consortium for R&D of laser and electron beam industrial application and process engineering, materials, methods and technologies of production- Research Centre of Trisaia, 75026 Rotondella (MT), Italy

[2]ENEA, Department for Sustainability of Production and Territorial Systems - Research Centre of Casaccia, 00123, Santa Maria di Galeria Rome, Italy

[3]Department of Industrial Engineering, University of Rome "Tor Vergata", 00133 Roma, Italy

[a]giuseppe.barbieri@enea.it, [b]francesco.cognini@enea.it, [c]massimo.moncada@enea.it, [d]antonio.rinaldi@enea.it, [e]gabriele.lapi@uniroma2.it

Keywords: Laser Welding, aluminum, wobbling, joining, tailored welded blank

Abstract.

The scope of this paper is to examine the improvement from laser welding by an innovative beam wobbling head towards the welding of tailored blanks parts, widely used in automotive to develop different stiffness aluminum components. For this purpose, butt joints and overlapping joints were produced from sheets made out of two industrial grades, i.e. AA-6082 T6 and AA-5754 H111 of different thickness. The technique was evaluated both with and without the use of a filler wire (AA-5556). The qualification of the welding process encompassed Non Destructive Testing (NDT) and mechanical testing. The results indicate that butt joints tend to fail within the base material (BM) of sheet with smaller thickness. On the contrary, the shear tests on lap joints highlighted a rupture mode occurring in the heat affected zone (HAZ) of the thin sheet. Remarkably, the wobbling process generally allows avoiding porosity when combined with an optimized set of welding parameters. Yet, a residual porosity was always detected in lap joints, varying with the size of the fused zone.

Introduction

Aluminum alloys in the automotive applications (BiW and /or bodycar) promise the reduction of the weight of the transport means and consequent increasing of the Well to Wheel efficiency. For passenger cars a weight reduction of 10 % reduces fuel consumption some 6 – 7 % with the direct consequence of a reduction of CO_2 emission. One of the challenge to extend the use of aluminum alloy is the availability of robust and efficient welding processes. Laser welding is the automotive production technology that promises better features in terms of quality and productivity in many instances [1,2]. Some of the challenges in laser welding of the aluminum alloys are associated with surface reflectivity, hot cracking, and porosity susceptibility, which can be overcome by laser welding processes deploying innovative beam wobbling heads [3,4]. In fact, the *key hole* rotation with the consequent mixing of the molten bath, can yield a reduction in the residual porosity. Furthermore, the addition of the right amount of filler wire material allows for a Mg content in the fused zone outside of the hot cracking range [5,6]. Both these features significantly improve the quality of welds and resulting components. The goal of the present work is to evaluate the capability of the commercial wobbling head for welding some standard automotive aluminum alloys in the more common joint configurations.

Materials

Sheets in AA-6082 T6 (2 mm thick) and AA-5754 H111 (1.5 mm thick) were used in the present work to produce butt and lap joints. The filler wire used in the process was the AA-5556 (diameter of 1 mm). The chemical compositions and the mechanical properties of all these alloys are summarized respectively in Table 1 and Table 2.

Table 1: Measured chemical compositions of aluminum alloys (UNI EN ISO 573-3).

Alloy Designation	Cr	Cu	Fe	Mg	Mn	Si	Ti	Zn	Others	
									Each	Total
AA-6082	0.25	0.10	0.50	0.60-1.2	0.40-1.0	0.70-1.3	0.10	0.20	0.05	0.15
AA-5754	0.30	0.10	0.40	2.6-3.6	0.50	0.40	0.15	0.20	0.05	0.15
AA 5556	0.10	0.10	0.40	4.7-5.5	0.5-1.0	0.25	0.10	0.25	0.05	0.15

Table 2: Measured mechanical properties of aluminum alloys (UNI EN 755-2).

Form Factor	Alloy	Temper	EN 755.2			Our Tests
			Rm [Mpa]	$R_{p0,2}$[Mpa]	A(%)	Rm [Mpa]
sheet	AA-6082	T6	>295	>250	>8	329
sheet	AA-5754	H111	>190	>80	>14	240
wire	AA-5556	As Welded	>240	>110	>17	-

Welding Process

The laser source used in our welding processing was an IPG Ytterbium Fiber Laser System (YLS-2000-CT-Y12), with an output power of 2300 W. The welding head comprises by a collimator, a wobble module, and a focusing lens, as shown in Fig.1 (left). The welding set-up is also shown in Fig.1 (right).

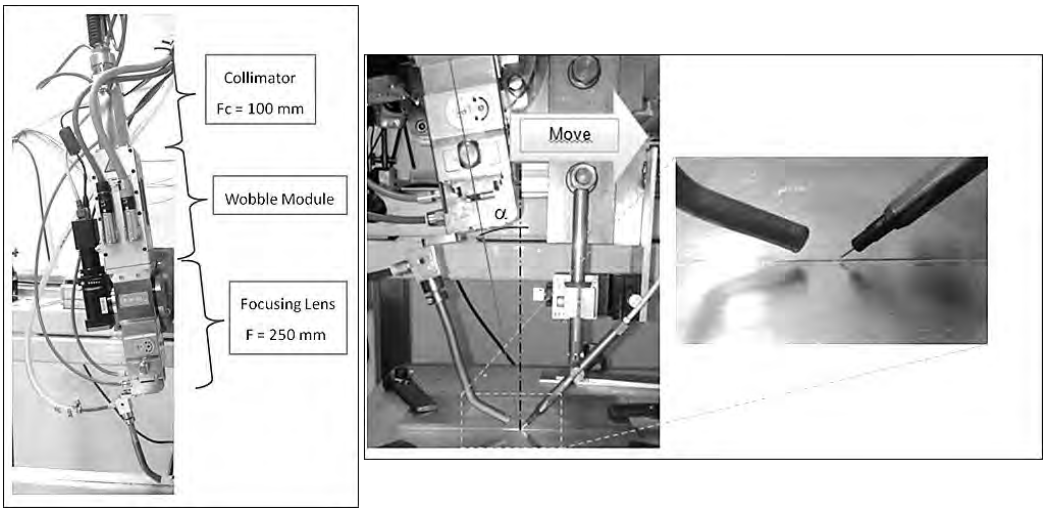

Fig.1, welding head constituted by a collimator, a wobble module and a focusing lens (left); welding set up (right).

The wobble module allows the controlled oscillatory rotation of the focal spot and the consequent mixing of the molten bath, thus reducing the welding porosity, which is the main

defectivity of aluminum laser welds. The maximum oscillation diameter here was about 2.9 mm and the oscillation frequency was up to 300 Hz.

Results and Discussion

Statistical Design of Experiments (DOE) was performed to optimize of the welding process [7, 8]. Using MINITAB16© a 2^3 factorial design with 3 factors and 2 levels was implemented. The investigated parameter (factors) were the influence of the welding speed (V), the laser output power (P), and the wobble amplitude (K). The output variables were the residual porosity and the shape of the welds cross-section. Other parameters were kept fixed, such as the frequency of wobble (200 Hz), the beam angle (10°), the focus position, and the gas process. The optimized welding parameters and the aspect of the cross-sections are summarized in Table 3, both for the butt and lap joints, both with and without filler wire.

Table 3: Optimized welding parameters for butt and lap joints and typical welds aspect.

Sample ID	Joints type	Parameters				Cross-Section	Set Up
		V (m/min)	P (W)	K	V_W (m/min)		
B	Butt	2	1500	6	No	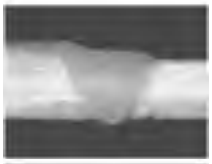	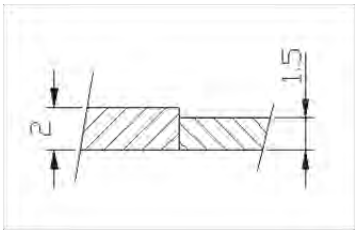
BW	Butt	3	2000	2	1.5	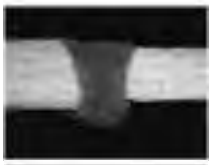	
L	Lap	1	1650	8	No	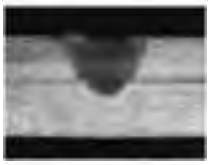	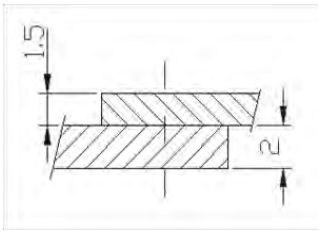
LW	Lap	1	1650	8	1	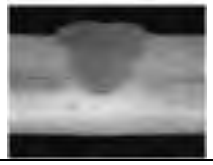	

Welds porosity was evaluated by digital radiography. The results, summarized in Fig.2: Digital radiography results: (left) samples a),b),c) with increasing porosity; (right) influence of the welding parameters on the cumulative area (mm^2) of porosity in 100 mm length welds for butt joints (up) and lap joints (down).Fig.2, demonstrated the effects of welding parameters on porosity. The plot in Fig.2 shows the total projected area of pores (in mm^2) as recorded by radiography of 100 mm welds.

Compared to the lap joints, the butt joints generally exhibited the lowest porosity. This likely happened because, in the fully penetration butt joints, the gases or the metal vapor generate during the key hole welding process can escape from the root side of the welds, while in the lap joints, due to the back solid state metal, this cannot occur.

The qualification of the welding process was done through micro hardness and tensile tests. An electro-mechanical machine (DMG, Denison Mayes Group) was used to conduct tensile tests in displacement controlled mode according to UNI EN ISO 6892-1. For the Lap Joint a custom shear test was been assessed in compliance with similar literature test [9]. Five "dogbone-shaped"

specimens were cut from each welded sample by water jet cutting and submitted for tensile testing. Representative results of the tensile tests on the butt joints and lap joints are shown in Fig.3.

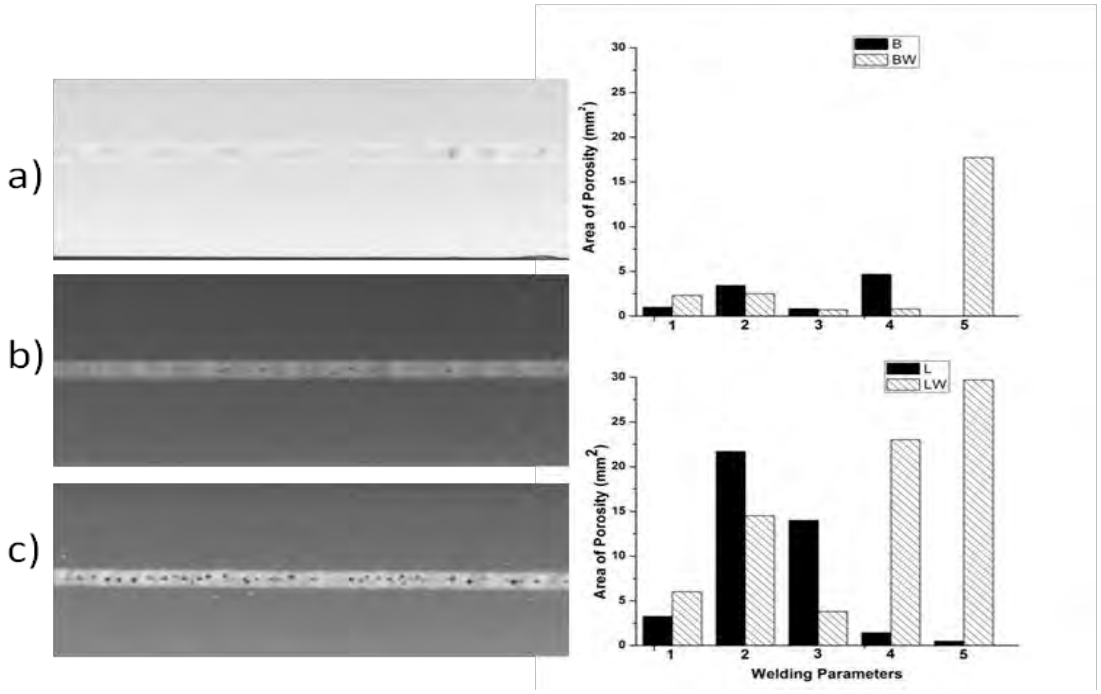

Fig.2: Digital radiography results: (left) samples a),b),c) with increasing porosity; (right) influence of the welding parameters on the cumulative area (mm^2) of porosity in 100 mm length welds for butt joints (up) and lap joints (down).

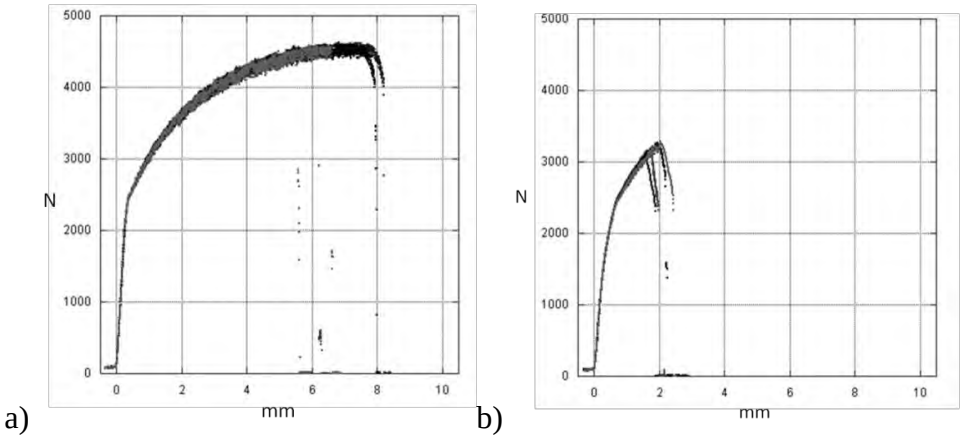

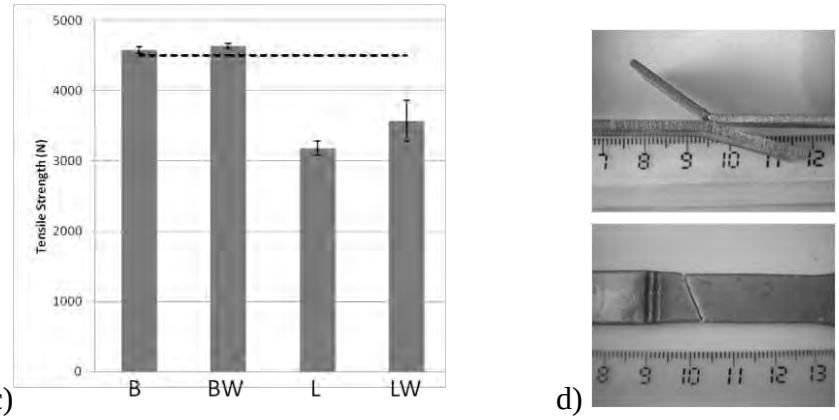

Fig.3: Results of the tensile tests on the butt joints (a) and the lap joints (b). The histogram (c) shows the tensile strength achieved for the butt joints with (BW) and without (B) filler wire, and for lap joints with (LW) and without filler wire (L); d) typical failure for the lap joints (up) and butt joints (down).

The dotted-line drawn in the histogram in Fig.3-c) marks the tensile strength of the base material AA 5754 H111 of the thinner side of the sample. Every butt joints exhibits high tensile strength values and the failure occurs at the level of the base material, only a few cases show the failure part in the base material and part in the HAZ, but the Rm is the same as in the former case. Lap joints exhibit a lower tensile strength, the failure occurring at the fused zone (FZ) mainly by shear stress: the sheets develop some local tilt to align their center planes this producing also a normal stress component at the interface (Fig. 4, right). The weld is therefore in a complex stress state with severe stress concentration. The same figure, at left, summarizes the lap joint strength results: it is correlated with weld width (as expected) and benefits from the filler material presence even if it causes a reduction in weld width.

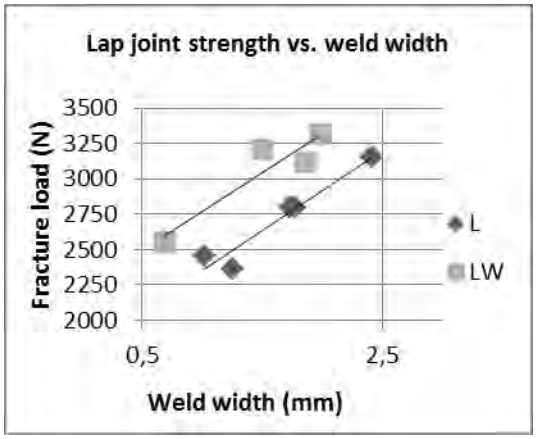

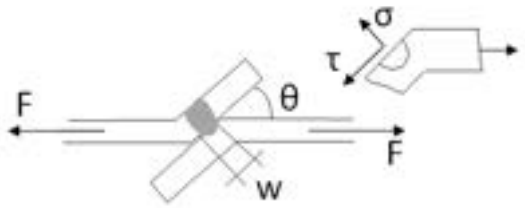

Fig. 4: lap joint strength (left), weld failure mode (right)

Micro hardness was evaluated through the cross-sections of both butt and lap joints with a micro Vickers hardness tester with test force of 200 gf and inter-distance between neighboring indentations of 0.2 mm. The hardness profiles for the butt and lap joints with and without the filler wire are shown in **Errore. L'origine riferimento non è stata trovata.**.

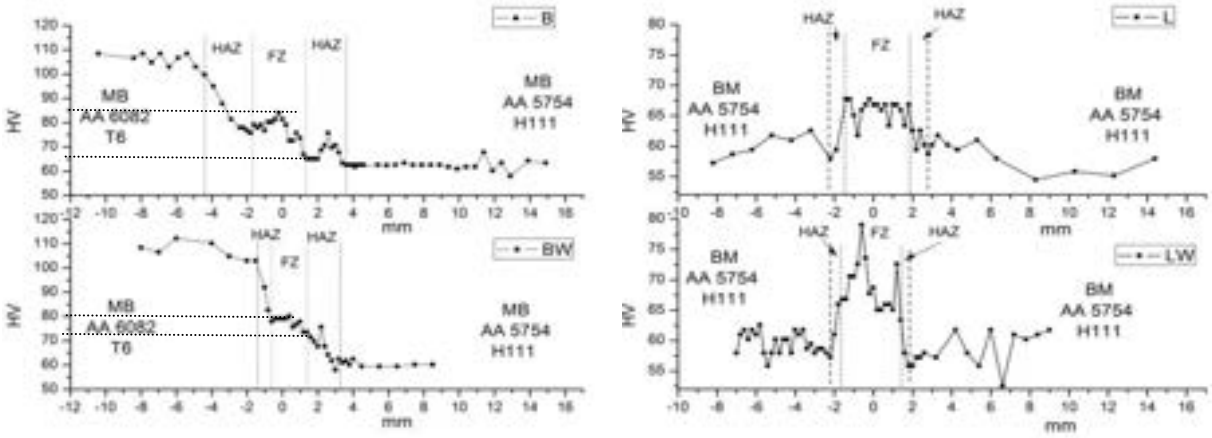

a) b)

Fig. 5: Micro hardness Vickers evaluated through the cross-sections of the butt joints (a) and the lap joints (b)

For the butt joints Fig. 5-a the hardness levels at the ends of the profiles are those of the base materials: AA-6082 T6 on the left side (about 108 HV) vs. AA-5754 H111 on the right side (about 60 HV). The width of the FZ is about 3 mm for the butt joint without the filler wire (the upper profile) and about 2.5 mm for that with the filler wire. The HAZ is smaller in the second case but, in both cases, the profile of the hardness along the FZ is little bit different due the dilution of the filler material, however the mean value are almost the same (about 75 HV). The lower value of the hardness is in the base material of the thinner sheet (AA-5754 H111). For the lap joints in Fig. 5-b, the hardness levels at the ends of the profiles are those of the base material (AA-5754 H111). The width of FZ is smaller in the case of the lap joint with filler wire and the hardness at the center of the FZ is quite bigger than the hardness in the sample without filler wire. The welding process with filler wire lead to the reduction of both HAZ and FZ, which can be attributed to the fact that part of the process heat is necessary to melt the filler wire, so the real amount of heat available to melt the BM result less that in the process without filler wire. In other word the filler wire cooling the melting pool.

Conclusions

The capability of the commercial wobbling head for welding standard automotive aluminum alloys AA-6082 T6 and AA-5754 H111 in the more common joint configurations was evaluated. The results show that, in the butt joints, the factors that influenced the porosity are the laser source power and the filler wire amount. Increasing the power and reducing the filler wire amount, lead to a reduction of porosity. A filler wire excess lead to a faster solidification of the molten bath that hinder the evacuation of the gases or the metal vapor generated during the welding process. This is the reason because to have a good quality joint we need to use more laser power to weld with filler wire. We realize the best welding parameter in terms of reduction of porosity with a Heat Input of 40 J/mm (BW) - 45 J/mm (B). In the range of variation of the parameters investigated in this work, for the butt joints, the wobbling variation doesn't affect the porosity. However, in terms of quality, productivity and efficiency the best parameters for butt Joint is the BW (Table 3) with a productivity of more than 30% and efficiency of 12,5% higher than B (Table 3). The effect of wobbling is more evident to increase the width of the strength section in the lap joint without increase the penetration depth. This is very useful to have a best surface appearance on the esthetic side. Moreover, a residual porosity remains in the lap joint due to the impossibility to evacuate completely the gas or metallic vapor generated during the laser processes for the intrinsic non fully penetrating welding. The shear tests demonstrated that, for the same other condition of welding, the mechanical features exhibit best strength using filler wire.

References

[1] Katayama, S., Handbook of laser welding technologies, (2013) Woodhead Publishing.

[2] Schweier, M., Spatter formation in laser welding with beam oscillation, (2013) Physics procedia, 41, pp. 20-30.

[3] Barbieri, G. et al., Mechanical behavior of aluminum sandwiches made by laser welding, (2015) Procedia Engineering, 109, pp. 427-434.

[4] Berend O, et al., High-frequency Beam Oscillating to Increase the Process Stability during Laser Welding with High Melt Pool Dynamics. LIA, editor. Proceedings of the 24th International Congress on Applications of Lasers & Electro-Optics, Orlando: LIA Pub; 2005, pp. 1032 1041

[5] Dausinger, F., Laser welding of aluminum alloys: from fundamental investigation to industrial application, (2000) Proc. SPIE 3888, 367.

[6] Yulong Zhang et al., Reduced hot cracking susceptibility by controlling the fusion ratio in laser welding of dissimilar Al alloys joints, (2015) J. Mater. Res., vol. 30, n. 7.

[7] Seyedmahmoud R, et al., 2015, "A primer of statistical methods for correlating parameters and properties of electrospun poly-L-lactide scaffolds for tissue engineering – PART 1: D.O.E". J Biomed Mater Res, 103(1), 91-102.
[8] Montgomery DC. Design and Analysis of Experiments. New York: Wiley; 2005.
[9] Miyazaki, Y., Furusako, S., Tensile shear strength of laser welded lap joints, (2007) Nippon Steel technical report, n. 95.

Atti del XXXIII Congresso Nazionale dell'Associazione

GRUPPO MISURE ELETTRICHE ED ELETTRONICHE

Benevento, 19 – 21 settembre 2016

SVILUPPO DI UN SISTEMA (SEMI)AUTOMATICO DI PROGETTAZIONE DI APPARECCHIATURE PER LA CONSERVAZIONE DI ALIMENTI ATTRAVERSO PEF

P. Casti[(1)], M. Salmeri[(1)], F. Bonfà[(2)], S. Ferrari[(2)], I. Bertini[(2)]
[(1)]Dip. di Ingegneria Elettronica, Università di Roma Tor Vergata, Via del Politecnico - 00173 Roma
[(2)] Unità Tecnica Efficienza Energetica, ENEA, C. R. Casaccia, Via Anguillarese 301 - 00123 Roma
mail autore di riferimento: salmeri@ing.uniroma2.it

1. INTRODUZIONE

Nell'industria alimentare, una peculiare importanza è rivestita dalle procedure di conservazione, in grado di prolungare per un ragionevole lasso di tempo la conservazione degli alimenti attraverso l'eliminazione o l'inattivazione di microrganismi e enzimi naturalmente in esso presenti dopo la sua preparazione e in grado di produrne il deterioramento. In particolare ci si riferisce a procedure di inattivazione microbica, intese come soppressione dell'attività funzionale di un microrganismo, cioè alla sua capacità di riprodursi e di produrre molecole o reazioni enzimatiche evidenti. Tali tecniche possono riferirsi all'intera popolazione di microrganismi o ad un suo sottoinsieme di microrganismi patogeni. L'attività batterica è regolata da diversi fattori ambientali, come la disponibilità di acqua, di nutrienti, di sostanze antimicrobiche naturali, il pH, l'umidità e la temperatura. Le tecniche di inattivazione microbica agiscono su uno o più di questi fattori rendendo più difficile o impossibile l'attività dei batteri [1].
In letteratura sono state studiate e sviluppate diverse tecniche di inattivazione, ciascuna delle quali ha proprie peculiarità riguardo alla tipologia di alimenti su cui è in grado di operare (per esempio liquidi o solidi), alla loro difficoltà di attuazione e alle conseguenze secondarie che esse possono avere sulle caratteristiche organolettiche del cibo sottoposto a trattamento. I microrganismi esposti ad un trattamento di inattivazione vengono inattivati secondo una cinetica di tipo esponenziale, la cui dinamica dipende dalle caratteristiche del trattamento e dei microrganismi stessi.
Nell'industria alimentare le tecniche di inattivazione microbica rappresentano una fase cruciale, sono eseguite attraverso macchinari specifici e richiedono una non indifferente energia per il loro funzionamento. Una tecnica molto promettente sotto numerosi punti di vista, non ultimo quello della sua efficienza energetica, ma tuttavia ancora in fase di studio, è quella dell'utilizzo dei campi elettrici pulsati (Pulsed Electric Fileds, PEF) come metodo non-termico di conservazione degli alimenti. Essa consiste nell'utilizzo di impulsi ad alta tensione, tipicamente 20 – 80 kV/cm, realizzati per mezzo di due elettrodi tra i quali si interpone l'alimento [1]. I vantaggi principali delle tecnologie PEF rispetto ai trattamenti termici tradizionali consistono nella migliore preservazione delle proprietà fisiche, nutrizionali e sensoriali del prodotto e nel limitato consumo energetico in assenza di scarti o fumi inquinanti, con conseguente riduzione dell'impatto ambientale di processo. Diversi lavori in questi ultimi anni hanno reso disponibili risultati teorici e sperimentali applicati a diverse tipologie di alimenti e utilizzanti apparecchiature ad hoc. Questi, se da un lato forniscono una base determinante per l'individuazione di adeguati percorsi di sviluppo dei sistemi PEF, dall'altro evidenziano una mancanza di organicità che, ad oggi, limita la generalizzazione dei risultati ottenuti e la diffusione delle metodiche proposte, ponendo importanti sfide di ricerca, sviluppo ed efficientamento energetico.

2. ATTIVITÀ DI RICERCA

La collaborazione dell'Unità di Ricerca di Roma Tor Vergata con l'ENEA si inserisce nel programma "Ricerca di sistema elettrico" che prevede un insieme di attività di ricerca e sviluppo finalizzate a ridurre il costo dell'energia elettrica per gli utenti finali, migliorare l'affidabilità del sistema e la qualità del servizio, ridurre l'impatto del sistema elettrico sull'ambiente e sulla salute e consentire l'utilizzo razionale delle risorse energetiche ed assicurare al Paese le condizioni per uno sviluppo sostenibile. Tale collaborazione scientifica si propone di esplorare l'applicabilità su vasta scala della tecnica di inattivazione batterica attraverso i PEF nel campo della conservazione degli alimenti in sostituzione delle attuali tecniche, più dispendiose da un punto di vista della efficienza energetica.
La prima fase di questo progetto che ha coperto questo ultimo anno è consistita nell'analisi di tipo quantitativo-descrittivo dello stato dell'arte in materia di PEF applicati alla conservazione degli alimenti, allo scopo di definire il target di analisi, identificando quali contributi considerare ed i criteri

di valutazione da adottare, soprattutto in relazione a sostenibilità ed efficienza energetica. È seguita dunque una sintesi delle prestazioni della metodica PEF mediante meta-analisi esplorativa. Utilizzando le informazioni estratte provenienti da studi e ricerche diversi, queste sono state integrate al fine di fornire le basi per l'impostazione di una metodologia multicriteriale e semiautomatica di supporto alla progettazione di apparecchiature PEF. A tale scopo, sono state applicate tecniche di tipo statistico sia a singoli studi che di tipo complessivo.

3. RISULTATI PRELIMINARI

L'analisi della letteratura scientifica internazionale in materia di conservazione degli alimenti mediante PEF ha evidenziato una mancanza di organicità e di uniformità nella descrizione dei parametri di processo, con informazioni rilevanti spesso mancanti. Il target di analisi identificato consiste in un gruppo di alimenti in forma liquida: acqua, latte, succhi di frutta, uovo liquido e vino. Tale scelta è volta a presentare la metodica PEF come alternativa, energeticamente vantaggiosa, alla pastorizzazione ed è sostanziata dalla efficacia dei PEF, comprovata da studi di laboratorio, proprio sugli alimenti liquidi menzionati, in virtù delle loro caratteristiche dielettriche. In aggiunta ai cibi solidi o densi, sono stati esclusi dal target le bevande gassate, come birra o vini frizzanti, o disomogenee per presenza di particolato, per le quali l'utilizzo dei PEF è ostacolato dalla formazione di archi elettrici.

Sono stati individuati due fattori di processo principali: l'intensità del campo elettrico E (in kV/cm) e la durata del tempo di trattamento T (in ms). Tali fattori sono i più importanti parametri di input responsabili dell'inattivazione dei microrganismi e la reperibilità dei loro valori, relativamente agli studi sperimentali analizzati, ha determinato la selezione degli studi stessi e l'inclusione dei dati sperimentali corrispondenti all'interno di una tabella integrativa. L'effetto sull'inattivazione è stato valutato in termini di riduzione logaritmica, log(S), ovvero come logaritmo del rapporto tra la concentrazione dell'agente microbico alla fine del trattamento e la concentrazione iniziale dello stesso agente. Il parametro S, quantificando l'efficacia del trattamento, fornirà l'output del sistema di supporto alla progettazione e sarà utile in fase di ottimizzazione. Ulteriori fattori di influenza in grado di influenzare la dinamica del processo di inattivazione sono stati aggiunti alla sintesi quantitativa realizzata: 1) tipologia e caratteristiche della camera di trattamento (statica o a flusso continuo, volume, etc.), 2) forma d'onda applicata (quadrata, esponenziale, etc.), 3) temperatura, 4) caratteristiche delle cellula microbiche (tipologia, morfologia, classificazione, etc.).

Su un campione di 42 studi selezionati e pubblicati dal 1980 al 2015, i valori medi (e deviazione standard) di E e T che sono risultati efficaci ai fini dell'inattivazione sono, rispettivamente, di 33 (15) kV/cm e 1,22 (3,46) ms, cui corrispondono valori di Log(S) uguali a 3,74 (2,13), ovvero una disattivazione percentuale superiore al 99,9 %. Le prestazioni variano in relazione ai parametri di influenza, ad esempio, i batteri Gram– , come l'Escherichia Coli, sono più sensibili ai PEF dei Gram+, in virtù della minore resistenza al campo elettrico generata dalla struttura delle loro membrane cellulari. A causa dell'elevato numero di parametri di influenza e della variabilità degli stessi vi è una evidente necessità di fornire una metodologia matematica per la pianificazione del trattamento PEF che garantisca che l'alimento trattato subisca condizioni elettriche tali da distruggere gli agenti patogeni in esso presenti. Il modello di Hülsheger [3], $S(E,T) = (T/T_c)\ \exp[-(E-E_c)/k]$, relaziona S ai valori di T ed E mediante la determinazione di tre parametri di regressione: il tempo ed il campo elettrico critici T_c ed E_c, ed una costante correttiva k, indicativa della suscettibilità del microrganismo al trattamento. Il modello stimato mediante regressione non lineare (T_c=1,7 ms, E_c=13,5 kV/cm e k=1.38) si è adattato bene ad un campione di 25 diversi dati sperimentali relativi a latte, succhi di frutta e uova liquide per l'inattivazione dell'Escherichia Coli, $R^2 = 0.76$, ponendo le basi per lo sviluppo di un sistema di progettazione per la conservazione di alimenti mediante PEF.

RIFERIMENTI BIBLIOGRAFICI

[1] Blackburn, C. and McClure, P.J., 2002. Foodborne pathogens: hazards, risk analysis and control. CRCPress.
[2] Mosqueda-Melgar, J., Elez-Martínez, P., Raybaudi-Massilia, R. M., and Martin-Belloso, O., 2008. Effects of pulsed electric fields on pathogenic microorganisms of major concern in fluid foods: a review. Critical reviews in food science and nutrition, 48(8), 747-759.
[3] Hülsheger, H., Potel, J., and Niemann, E. G., 1983. Electric field effects on bacteria and yeast cells. Radiation and environmental biophysics, 22(2), 149-162.